

Mitochondria and neuronal activity

Oliver Kann and Richard Kovács

Am J Physiol Cell Physiol 292:641-657, 2007. First published Nov 8, 2006;
doi:10.1152/ajpcell.00222.2006

You might find this additional information useful...

This article cites 219 articles, 95 of which you can access free at:

<http://ajpcell.physiology.org/cgi/content/full/292/2/C641#BIBL>

This article has been cited by 2 other HighWire hosted articles:

Gamma Oscillations and Spontaneous Network Activity in the Hippocampus Are Highly Sensitive to Decreases in pO₂ and Concomitant Changes in Mitochondrial Redox State

C. Huchzermeyer, K. Albus, H.-J. Gabriel, J. Otahal, N. Taubenberger, U. Heinemann, R. Kovacs and O. Kann

J. Neurosci., January 30, 2008; 28 (5): 1153-1162.

[\[Abstract\]](#) [\[Full Text\]](#) [\[PDF\]](#)

LETM1, deleted in Wolf Hirschhorn syndrome is required for normal mitochondrial morphology and cellular viability

K. S. Dimmer, F. Navoni, A. Casarin, E. Trevisson, S. Ende, A. Winterpacht, L. Salviati and L. Scorrano

Hum. Mol. Genet., January 15, 2008; 17 (2): 201-214.

[\[Abstract\]](#) [\[Full Text\]](#) [\[PDF\]](#)

Updated information and services including high-resolution figures, can be found at:

<http://ajpcell.physiology.org/cgi/content/full/292/2/C641>

Additional material and information about *AJP - Cell Physiology* can be found at:

<http://www.the-aps.org/publications/ajpcell>

This information is current as of March 7, 2008 .

Mitochondria and neuronal activity

Oliver Kann and Richard Kovács

Institute for Neurophysiology, Charité-Medical University of Berlin, Germany

Kann O, Kovács R. Mitochondria and neuronal activity. *Am J Physiol Cell Physiol* 292: C641–C657, 2007. First published November 8, 2006; doi:10.1152/ajpcell.00222.2006.—Mitochondria are central for various cellular processes that include ATP production, intracellular Ca²⁺ signaling, and generation of reactive oxygen species. Neurons critically depend on mitochondrial function to establish membrane excitability and to execute the complex processes of neurotransmission and plasticity. While much information about mitochondrial properties is available from studies on isolated mitochondria and dissociated cell cultures, less is known about mitochondrial function in intact neurons in brain tissue. However, a detailed description of the interactions between mitochondrial function, energy metabolism, and neuronal activity is crucial for the understanding of the complex physiological behavior of neurons, as well as the pathophysiology of various neurological diseases. The combination of new fluorescence imaging techniques, electrophysiology, and brain slice preparations provides a powerful tool to study mitochondrial function during neuronal activity, with high spatiotemporal resolution. This review summarizes recent findings on mitochondrial Ca²⁺ transport, mitochondrial membrane potential ($\Delta\Psi_m$), and energy metabolism during neuronal activity. We will first discuss interactions of these parameters for experimental stimulation conditions that can be related to the physiological range. We will then describe how mitochondrial and metabolic dysfunction develops during pathological neuronal activity, focusing on temporal lobe epilepsy and its experimental models. The aim is to illustrate that 1) the structure of the mitochondrial compartment is highly dynamic in neurons, 2) there is a fine-tuned coupling between neuronal activity and mitochondrial function, and 3) mitochondria are of central importance for the complex behavior of neurons.

brain slice preparation; electrophysiology; NADH; mitochondrial calcium transport; temporal lobe epilepsy

MITOCHONDRIA ARE UNIQUE ORGANELLES providing the host cell with ATP by oxidative phosphorylation. Mitochondria are also central to intracellular Ca²⁺ homeostasis, steroid synthesis, generation of free radical species, and forms of apoptotic cell death. As a consequence, mitochondrial dysfunction has devastating effects on the integrity of cells and may thus be critically involved in aging, metabolic and degenerative diseases, as well as cancer in higher organisms and humans (218).

Most of the studies on mitochondrial function have been conducted in preparations of isolated mitochondria and dissociated cultures of excitable and nonexcitable cells. Data from these studies have been summarized and discussed in a variety of excellent general reviews on mitochondrial genetics, biochemistry, physiology, and pathology, characterizing mitochondria as a highly dynamic, sensitive, but potentially harmful entity (15, 24, 55, 80, 145, 179).

The central nervous system (CNS) has an extraordinary high metabolic rate, as it consumes about 20% of oxygen inspired at rest, while accounting for only 2% of the body weight (199). This immense metabolic demand is because neurons are highly differentiated cells that need large amounts of ATP for maintenance of ionic gradients across the cell membranes and for neurotransmission. Since most neuronal ATP is generated by

oxidative metabolism, neurons critically depend on mitochondrial function and oxygen supply (1, 60, 144). Conversely, neuronal function and survival are very sensitive to mitochondrial dysfunction (62, 158). The second important aspect is the functional heterogeneity in neuronal segments, which is also reflected by the complex morphology of neurons, which can extend over hundreds of micrometers, depending on neuronal cell type and brain region. Accordingly, dendritic, somatic, axonal, and presynaptic segments of neurons might have quite different energy demands, which require local adaptation of energy supply, as well as local cellular signals interconnecting neuronal and mitochondrial metabolic activity. For these reasons, the detailed description of the interplay between mitochondrial function, energy metabolism, and neuronal activity is of critical importance for understanding of neuronal physiology and pathophysiology in various neurological diseases (101, 187, 193). However, the exploration of this interplay in intact animals is aggravated by a variety of factors, like restriction of investigations to cortices of cerebrum and cerebellum, limited control over stimulation parameters, complicated recording conditions (e.g., dye loading with fluorescence indicators), as well as artifacts resulting from breathing and changes in blood flow in vivo. To bypass these limitations, most of the recent studies in the field have been performed in vitro. The isolated nerve terminal (synaptosome preparation) is very suitable for exploring mitochondrial bioenergetics in a physiological milieu, and dissociated neuronal cell cultures

Address for reprint requests and other correspondence: O. Kann, Institut für Neurophysiologie, Charité-Universitätsmedizin Berlin, Tucholskystrasse 2, 10117 Berlin, Germany (e-mail: oliver.kann@charite.de).

provide eased access for patch-clamp, imaging, and pharmacological studies. However, the significance of the data for mitochondrial function in intact neurons of the postnatal brain is limited to a certain degree because synaptosomes represent a small fraction of neurons and neuronal cell cultures are derived from embryos. From the experimental point of view, the combination of brain slice preparations, new imaging techniques with high spatiotemporal resolution, and electrophysiology provides an alternative and powerful tool for studying mitochondrial function and energy metabolism during neuronal activity on the tissue level, as well as on the level of dendrites, axons, and somata. Slice preparations may experience brief hypoxic periods during preparation and rely on diffusion of nutrients and oxygen from the bath solution. Nevertheless, the great advantages in combining these methods are minimal invasiveness of imaging techniques, high-speed electrophysiological monitoring of neuronal activity, as well as preservation of neurons in their three-dimensional expansion and natural interaction with glial cells in brain slices, which is very close to the *in vivo* situation. Moreover, slice preparations allow experimental access to virtually any structure of the brain and can be made from embryonic, juvenile, and adult (aged) animals.

In this review, we will summarize and discuss recent findings on mitochondrial function and energy metabolism during neuronal activity, when stimulation paradigms are restricted to the physiological range. Because of the advantages mentioned above, we will focus on studies that were conducted in brain slice preparations and relate them to findings from *in vivo*, synaptosomes, or dissociated neuronal cultures, when suitable. We will then discuss how mitochondrial and metabolic dysfunction develops during pathological neuronal activity, focusing on temporal lobe epilepsy (TLE) and its experimental models.

GENERAL ASPECTS

Structure, Distribution, and Bioenergetics of Brain Mitochondria

Mitochondria are formed by two membranes that may have contact sites. The outer membrane is permeable for ions and small molecules, and its permeability is possibly well regulated. In the intermembrane space important enzymes like creatine kinase and holocytochrome *c* are located. The inner mitochondrial membrane is almost impermeable, thus forming a tight barrier between the mitochondrial matrix and the neuronal cytoplasm, and is equipped with a variety of ion channels and transporters, like the Ca^{2+} uniporter, K^+ ATP channels, and $\text{Na}^+/\text{Ca}^{2+}$ exchanger, as well as mitochondrial enzyme systems like the electron transport chain (ETC). Mitochondria are thought to arise from the cell soma (47) and usually form a dynamic network (154, 225). Due to complex and perhaps special cytoskeletal transport mechanisms, individual mitochondria are highly mobile in anterograde and retrograde directions in neurons (88). Therefore, neuronal mitochondria can be positioned and retained in neuronal segments with high metabolic demand, like active growth cones and pre- and postsynaptic structures (128, 182).

Brain mitochondria primarily utilize pyruvate from cytoplasmic glycolysis to reduce nicotinamide adenine dinucleotides and flavin adenine dinucleotides by enzymes of the Krebs-

Szent-Györgyi cycle (tricarboxylic acid cycle, TCA). NADH and FADH_2 serve in energy transfer to the ETC, which consists of complex I (NADH ubiquinone oxidoreductase), complex II (succinate dehydrogenase), complex III (ubiquinol cytochrome *c* oxidoreductase), and complex IV (cytochrome *c* oxidase). Via these complexes, electrons are transferred from NADH and FADH_2 to O_2 . The reactions of complexes I, III, and IV also imply the transfer of protons from the mitochondrial matrix to the intermembrane space, which establishes a potential difference ($\Delta\Psi_m$) of 150–180 mV (negative with respect to cytosol) across the inner mitochondrial membrane. Thus, $\Delta\Psi_m$ sets the driving force for protons (together with ΔpH) that actuate F_1F_0 -ATP synthase (complex V) to generate ATP and for cytosolic Ca^{2+} ions to accumulate in the matrix via the mitochondrial Ca^{2+} uniporter (74, 151) (Fig. 1). The current concept on regulation of mitochondrial oxidative metabolism is primarily based on studies of isolated mitochondria or mitochondrial enzymes. It implicates regulatory functions of substrates like the ratio of ADP/ATP, as well as changes in the mitochondrial calcium concentration ($[\text{Ca}^{2+}]_m$), which has been shown to stimulate the activity of TCA cycle dehydrogenases and to functionally modulate complexes IV and V (80, 99, 145). Recent studies applying physiological Ca^{2+} -mobilizing stimuli in nonexcitable cells and myocytes strongly support this concept (79, 178, 222).

Mitochondrial Ca^{2+} Transporters and Channels

Net mitochondrial Ca^{2+} transport depends on the relative rates of Ca^{2+} uptake and extrusion. The main Ca^{2+} uptake pathway is the mitochondrial Ca^{2+} uniporter, which is allosterically activated by Ca^{2+} , giving rise to a Hill coefficient of 2 (15, 76). Although the exact molecular nature of the Ca^{2+} uniporter has not been determined (15), a recent patch-clamp study in mitoplasts suggests that it is likely an inwardly rectifying Ca^{2+} -selective ion channel (Ref. 109; see also Refs. 76, 134). Mitochondrial Ca^{2+} uptake was already observed in intact cells at cytosolic calcium concentrations ($[\text{Ca}^{2+}]_c$) as low as 150–300 nM (173). However, high local Ca^{2+} domains of tens of micromolar in the vicinity of voltage-operated Ca^{2+} channels or Ca^{2+} release sites of the endoplasmic reticulum (183) might be necessary for fast $[\text{Ca}^{2+}]_m$ transients (71, 164). During pathological elevations in $[\text{Ca}^{2+}]_c$, mitochondria virtually use the full respiratory capacity to accumulate Ca^{2+} (76). Since mitochondria have been found to more effectively translate oscillations than sustained elevations in $[\text{Ca}^{2+}]_c$ into metabolic responses, the presence of an inactivating Ca^{2+} uptake mode has been suggested (Ref. 79; see also Ref. 204). Resting free $[\text{Ca}^{2+}]_m$ has been found to be as low as $[\text{Ca}^{2+}]_c$, in spite of the considerable electrochemical gradient for Ca^{2+} (8), which reflects the activity of Ca^{2+} extrusion mechanisms, as well as the high mitochondrial Ca^{2+} buffer capacity likely due to formation of Ca^{2+} phosphate complexes that have been suggested to represent a reversible Ca^{2+} store (45, 175). For translating small $[\text{Ca}^{2+}]_c$ transients to mitochondria, the Ca^{2+} -binding aspartate-glutamate carrier aralar has been proposed recently (166).

In excitable cells, the main mitochondrial Ca^{2+} extrusion pathway is the $\text{Na}^+/\text{Ca}^{2+}$ exchanger, which is responsible for low resting $[\text{Ca}^{2+}]_m$. This transporter was previously thought to exchange one Ca^{2+} ion with two incoming Na^+ ions (20).

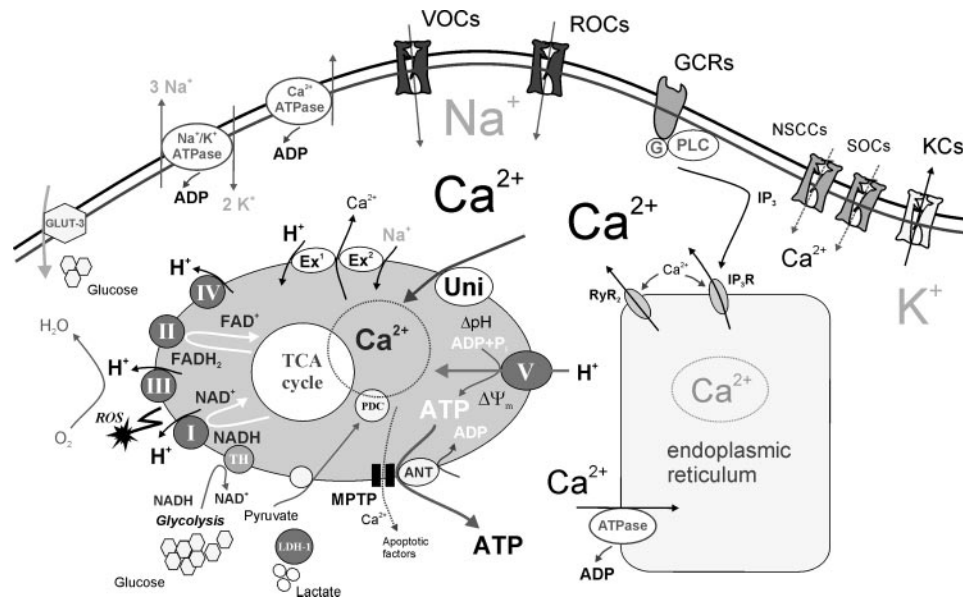


Fig. 1. Neuronal activity is associated with Ca^{2+} entry via voltage-operated channels (VOCs), receptor-operated channels (ROCs), store-operated channels (SOCs), and nonselective cation channels (NSCCs), as well as with Ca^{2+} release from endoplasmic reticulum via receptors for inositol (1,4,5)-trisphosphate (IP_3 R) and ryanodine (RyR). IP_3 is generated via activation of G-protein coupled receptors (GCRs) and phospholipase C (PLC). To maintain ionic gradients across the neuronal membrane, Na^+ - K^+ -ATPase and Ca^{2+} -ATPases consume large amounts of ATP. Mitochondria take up Ca^{2+} in the vicinity to sites of Ca^{2+} influx and/or Ca^{2+} release via the mitochondrial Ca^{2+} uniporter (Uni). Glycolysis and lactate dehydrogenase-1 (LDH-1) provide NADH and pyruvate that is transferred to the mitochondrial matrix and converted by pyruvate dehydrogenase complex (PDC) to fuel the tricarboxylic acid (TCA) cycle. NADH and FADH transfer energy from the TCA cycle to complex I and complex II of the electron transport chain (ETC), respectively. Activity of the ETC establishes a potential (150–180 mV negative to cytosol, $\Delta\Psi_m$) and a proton gradient (ΔpH) across the inner mitochondrial membrane, setting a driving force for protons to actuate complex V (ATP synthase), for calcium and for transporters like adenine nucleotide translocase (ANT). The activity of TCA cycle enzymes and PDC is stimulated by Ca^{2+} (overlap in circles). Generation of reactive oxygen species (ROS) occurs at complexes I and III, as well as α -ketoglutarate dehydrogenase in the TCA cycle. Further abbreviations: GLUT-3 (glucose transporter-3), TH (nicotinamide nucleotide transhydrogenase), MPTP (mitochondrial permeability transition pore), Ex^1 (H^+ / Ca^{2+} exchanger), Ex^2 (Na^+ / Ca^{2+} exchanger), KCs (potassium channels).

Other studies proposed the stoichiometry of three Na^+ for one Ca^{2+} ion; thus the exchanger would mediate electrogenic Ca^{2+} extrusion (12, 98). Due to its low capacity, the transport rate of this exchanger can be surpassed by the Ca^{2+} uniporter, leading to net Ca^{2+} accumulation in mitochondria. The mitochondrial H^+ / Ca^{2+} exchanger is the second extrusion pathway, which is slow and saturates at a lower $[\text{Ca}^{2+}]_c$ than the Na^+ / Ca^{2+} exchanger. Thus its contribution to fast mitochondrial Ca^{2+} cycling is limited (15, 75). An alternative pathway for Ca^{2+} efflux is transient low-conductance opening of the mitochondrial permeability transition pore (MPTP), which might save mitochondria from toxic Ca^{2+} loads (92, 230).

Neuronal Activity, Energy Metabolism and Neuronal-Astrocytic Interactions

Repetitive action potential firing causes accumulation of Na^+ , Ca^{2+} , and Cl^- in the neuronal cytosol and the release of K^+ to the extracellular space (86, 159). Elevations in the extracellular potassium concentration ($[\text{K}^+]_o$) are reversed by ATPase activity and K^+ buffering of astrocytes (156).

To maintain ionic gradients and thus neuronal excitability, the activity of ion transport processes, namely Na^+ - K^+ -ATPases and Ca^{2+} -ATPases, increases. These processes cover about 60–80% of ATP consumption in the CNS. Another 10–20% is consumed by neurotransmission, which includes synthesis and packaging of neurotransmitters in vesicles and the transport to presynaptic endings (1, 61). The major energy substrate for mitochondrial oxidative metabolism is glucose (38, 198). Under physiological conditions, facilitated diffusion

of glucose via the GLUT-1 transporter across the blood-brain barrier to the parenchyma is more rapid, compared with other oxidizable substrates such as lactate, keto acids, fatty acids, and amino acids (167). Although neuronal dendrites and axons have sparse contact with capillaries, neurons are well equipped to metabolize glucose. This is because brain glucose levels are evenly distributed between intracellular and extracellular compartments, and neurons possess high levels of glycolytic enzymes, as well as the fast glucose transporter, GLUT-3 (124, 171). By using lactate dehydrogenase-1, neurons might also derive pyruvate from lactate, which can be provided by astrocytic anaerobic glycolysis (139) (Fig. 1).

The interactions between neurons and astrocytes are not restricted to a putative energy supply with lactate. Astrocytes are also central for provision of precursors and other substrates to neurons, regulation of extracellular ion homeostasis, transport and metabolism of neurotransmitters, ammonia detoxification, and volume regulation (161, 188, 200). The underlying structural prerequisites of astrocytes are formation of an elaborated astrocytic network via gap junctions, close contacts to capillaries, and enwrapment of synapses.

MEASUREMENTS OF MITOCHONDRIAL FUNCTION IN BRAIN SLICES

Brain Slice Preparations

Acute brain slices. The most frequently used preparation to study fundamental principles in neurons and neuronal networks is the acute brain slice from mouse, rat, or even human brain

specimens (127, 195). In this preparation, brain tissue is cut in slices of 300–500 μm thickness (101, 133, 150). To minimize ischemic (anoxic) neuronal damage due to arrest of blood circulation, the preparation of brain slices is carried out quickly in ice-cold artificial cerebrospinal fluid (ACSF). ACSF usually contains ion concentrations comparable to the cerebrospinal fluid in vivo (19, 85). Notably, for investigations of brain slices much higher glucose concentrations (10–26 mM) are used compared with the brain in vivo (0.35–2.6 mM; summarized by Ref. 126) because it is difficult to obtain healthy slices using lower concentrations. It has been speculated that high glucose levels get converted to lactate, which might support recovery from hypoxic events, e.g., during brain slicing (194). Oxygenation and pH adjustment of ACSF is achieved by a mixture of 95% O_2 and 5% CO_2 (carbogen). This is because many cells in the upper and lower 50 μm of the slice are damaged by the vibrating blade, and a sufficient oxygen supply for healthy neurons in the slice core ultimately depends on a steep O_2 diffusion gradient. At 95% ambient O_2 and under interface recording conditions (slice maintained on the ACSF surface), tissue oxygen tension (P_{O_2}) was determined, with values of around 700 mmHg at the surface and around 300 mmHg at a depth of 265 μm in acute hippocampal slices (400 μm thickness), which rapidly declined during repetitive electrical stimulation of the tissue (65). These values can be significantly lower in slices maintained under submerged recording conditions because of the limiting factors of O_2 solubility, perfusion speed of ACSF, and a normal atmosphere above the bath chamber. These aspects on glucose and O_2 supply have to be kept in mind when interpreting data from brain slice preparations. Hyperoxic conditions, for example, might contribute to experimental artifacts in the uppermost cell layers of a slice. Nevertheless, hyperoxic conditions also exist when investigating isolated mitochondria or dissociated neuronal cultures at ambient P_{O_2} levels. After the cutting procedure, brain slices are allowed to recover and equilibrate to ACSF for 1–2 h, which reverses neuronal and mitochondrial swelling (211).

Organotypic slice cultures. In organotypic slice cultures from hippocampus or cortex (112, 207), neurons and glial cells largely maintain morphology, histological architecture, and their natural interactions (“organotypic”) (228). In both rats and mice, organotypic slice cultures can be prepared from embryonic states up to postnatal day 16. Brain slices (400 μm) are usually prepared from pups under sterile conditions and then maintained on Biopore membranes in interface conditions for up to 4 wk using standard incubators (5% CO_2 , 20% O_2 , 36°C). The medium also contains high glucose levels (10 mM and more) and a serum component (up to 25%) that supports recovery after cutting. Within days in vitro, slice cultures get thinner to 150–200 μm , corresponding to 10- to 12-cell layers (9), which reduces the diffusion distances for O_2 , ions, and drugs compared with acute slices. Under interface conditions with 20% ambient O_2 , P_{O_2} values of 120 mmHg at the surface and 67 mmHg at a depth of 100 μm were determined at rest (176), the latter of which is closer to in vivo data obtained under normoxic conditions in the rat brain (217). Notably, slice cultures mature in vitro, and synaptic components like glutamate receptors are stably maintained (9), whereas aberrant synaptic reorganization occurs to a variable degree in long-term cultures (78).

Experimental Induction and Monitoring of Neuronal Activity

In brain slice preparations, neuronal activity can be reliably evoked by application of electrical stimulation, neurotransmitters, or pharmacology. For electrical stimulation, single pulses (0.1 ms) are repetitively applied at frequencies up to 100 Hz and with train durations in the range of seconds (21, 102). Alternatively, neurotransmitters and exogenous receptor ligands like glutamate or carbachol are dissolved in ACSF and applied using the superfusion system or a pressure device for brief, local application (103, 197). For induction of pathological epileptiform neuronal activity, a variety of tools exist. Omission of Mg^{2+} ions from ACSF results in hyperexcitability and manifestation of epileptiform activity in brain slice preparations because of removal of the Mg^{2+} ion blockade from *N*-methyl-D-aspartate (NMDA) receptors, removal of the surface discharge screening, and increased transmitter release probability (“low Mg^{2+} model”; Ref. 152). Further common pharmacological tools are reduction of synaptic inhibition by use of the GABA receptor antagonists, bicuculline and picrotoxin, and/or depolarization of neurons using 4-aminopyridine, or an elevated extracellular potassium concentration ($[\text{K}^+]_o$) in ACSF (69).

Patch-clamp recordings in the whole-cell or cell-attached configuration allow for precise monitoring of membrane currents or membrane potential changes in individual neurons (112, 150). Extracellular recording electrodes are used to monitor the evoked field potential from a large number of neurons neighboring the recording site. Shape and amplitude of field potentials allow judgment of the type and degree of neuronal activity and serve as a reference parameter to adjust, for example, the intensity for electrical stimulation (65, 69). An additional parameter is provided when using double-barreled, ion-sensitive microelectrodes. K^+ -sensitive electrodes, for example, record changes in $[\text{K}^+]_o$ (138). Transient increases in $[\text{K}^+]_o$ of 2 to 3 mM from basal levels occur during physiological neuronal activity in vivo (2, 84). By contrast, during pathological neuronal activity like seizures or spreading depression, $[\text{K}^+]_o$ can increase up to tens of millimolar in vivo (52). Thus electrophysiological monitoring of $[\text{K}^+]_o$ can be used as an accurate parameter to judge the degree of evoked neuronal activity in brain slice preparations (102, 125).

Fluorescence Monitoring of Mitochondrial Parameters in Brain Slices

A variety of tools and methods exist to monitor mitochondrial parameters. Here, we will briefly discuss the most common fluorescence parameters, when used in brain slice preparations. For technical details and properties of fluorescence probes, the reader is referred to manufacturers and other reviews (94, 158, 231).

NADH and FAD fluorescence have been studied in vivo and in brain slice preparations to monitor changes in cellular energy metabolism (21, 102, 103, 144). When excited with ultraviolet light (340 nm and 360 nm, for NADH and NADPH, respectively) the reduced forms, NADH and NADPH, fluoresce at 450 nm, while the oxidized forms are nonfluorescent (3). Investigators often refer to changes in NAD(P)H fluorescence because the emission spectra of NADPH and NADH overlap, and their redox states are coupled via the activity of the nicotinamide nucleotide transhydrogenase. However,

NADPH levels were found to be low in brain tissue (36, 104, 111).

NAD(P)H fluorescence in brain slices is primarily governed by mitochondrial activity of the electron transport chain and the TCA cycle. Under certain conditions, it might be also influenced by extramitochondrial signaling and antioxidative processes, where NADH and NADPH serve as cofactors (14, 54, 110). Moreover, in astrocytes with high glycolytic activity, cytosolic NAD(P)H might significantly contribute to the overall NAD(P)H fluorescence (105). Thus NAD(P)H fluorescence and its changes in brain slice preparations are influenced by a variety of factors and have to be interpreted with care (190).

Electron transport flavoproteins and α -lipoamide dehydrogenase contribute to about 75% of the flavin fluorescence in neurons (90, 121). Since both of them are also closely linked to the mitochondrial NADH system, monitoring changes in FAD fluorescence gives insights into the mitochondrial redox state (180, 197). Because here the oxidized form is fluorescent, changes in FAD fluorescence are opposite to NAD(P)H fluorescence. Although FAD fluorescence is weaker than NAD(P)H fluorescence, it has the advantage of an excitation maximum at 450 nm, allowing prolonged recordings in brain slice preparations, due to less phototoxicity.

For determining changes in $\Delta\Psi_m$, membrane-permeant cationic fluorescence indicators, like rhodamine 123, are used that show a Nernstian distribution at the polarized mitochondrial inner membrane and accumulate within the matrix. There are basically two experimental approaches for monitoring changes in $\Delta\Psi_m$ (157). When dye concentrations in the bath are in the micromolar range, mitochondria accumulate three to four orders of magnitude higher dye concentrations, leading to significant self-quenching of the fluorescence. Mitochondrial depolarization results in a release of the dye with subsequent unquenching in surrounding cytosol and the matrix, resulting in a net fluorescence increase. Conversely, if nanomolar dye concentrations are used for the staining, intramatrix quenching is negligible, and mitochondrial depolarization leads to a decrease of the mitochondrial fluorescence (231). Although the latter method is more tolerable for the cells (see below), brief loading periods with high dye concentrations have been found useful in brain slice preparations to reach fast dye equilibrium and to take advantage of the signal amplification due to unquenching (17, 114). The execution and interpretation of experiments with these cationic dyes in slice preparations require special attention because the geometry of cellular compartments is highly heterogeneous, the extracellular space is very small (7–16% of the tissue; Ref. 137), compared with dissociated cell cultures, and ACSF exchange is variable when comparing slice surface with core. These factors might significantly influence dye distribution and fluorescence signal kinetics (see also Ref. 158). In our hands, rhodamine 123 bulk loading in the micromolar range leads to bright mitochondrial and weak cytosolic staining, when applying confocal imaging in organotypic slice cultures. During neuronal activation, a significant increase in fluorescence occurs in the cytosol, reflecting dye release from mitochondria and subsequent unquenching. Although it is hard to resolve the extracellular space in confocal images, the contribution of changes in extracellular fluorescence is relatively low due to the volume ratio between cytosol and extracellular space. Once released into the cytosol, however, dye reuptake by repolarizing mito-

chondria competes with dye loss due to plasma membrane depolarization. Thus changes in plasma membrane potential might shape the recovery phase of the signal. It should be also stressed that rhodamine dyes are photosensitizers and potentially form reactive oxygen species (ROS) upon excitation, which might significantly influence mitochondrial function (91).

For determining mitochondrial free radical production, fluorescence probes like hydroethidine (HET) and 4-amino-5-methylamino-2',7'-difluorofluorescein (DAF-FM) are used. These molecules are nonfluorescent in their reduced form, but fluoresce after oxidation. The dyes show some preference for a specific free radical. For example, HET was shown to be selectively oxidized by superoxide radicals (18), and DAF-FM has been used for detection of nitric oxide (NO) (26, 189). Unfortunately, the selectivity of the dyes that can be acquired in cell-free systems does not necessarily apply to the cellular environment, where compartmentalization and local redox conditions might influence the reaction. In case of several dyes (HET, dihydrorhodamine), mitochondrial accumulation of the oxidation end-products and subsequent release due to depolarization of mitochondrial membranes might result in false-positive results (30). Therefore, studies on free radical formation in brain slices always require both positive and negative controls (189).

Mitochondria-specific, Ca^{2+} -chelating fluorescence probes, like rhod-2 and rhod-FF, are positively charged in their membrane-permeant, acetoxymethyl ester form and thus accumulate in mitochondria. After cleavage of the ester bond, the dye becomes fluorescent, Ca^{2+} sensitive, and trapped in the organelles. Nevertheless, de-esterification of the dye already occurs in the cytosol, and therefore, a part of the fluorescence signal represents changes in $[\text{Ca}^{2+}]_c$. Although the cytosolic part of the signal can be decreased by applying appropriate dye-loading protocols, control experiments with pharmacological means are required in brain slice preparations (102). Another option for discrimination between cytosolic and mitochondrial fluorescence fractions is the use of spatial frequency filtering of recorded fluorescent images (71, 72, 112). This takes advantage of the fact that the cytosolic dye content gives rise to a smooth, slow, spatial frequency component, whereas mitochondria are represented at high spatial frequencies due to their small size. Another elegant way to decrease cytosolic fluorescence is the application of the dye in acetoxymethyl ester form through a patch pipette, which results in mitochondrial accumulation of the cleaved dye and dilution of the de-esterified dye in the cytosol by the large amount of leuco dye from the pipette (16). The dyes listed above measure free Ca^{2+} . Therefore, when considering total Ca^{2+} , it should be taken into account that the Ca^{2+} buffer capacity of mitochondria is several orders of magnitude higher than the cytosol (8).

MITOCHONDRIAL FUNCTION DURING PHYSIOLOGICAL NEURONAL ACTIVITY

Transient Increases in $[\text{Ca}^{2+}]_m$ During Synaptic Activity

Neuronal activity is associated with transient elevations in $[\text{Ca}^{2+}]_c$ due to Ca^{2+} entry via the plasma membrane and Ca^{2+} release from intracellular stores. Ca^{2+} entry is mediated by voltage-operated Ca^{2+} channels, receptor-operated and store-operated Ca^{2+} channels, or nonselective cation channels (4, 10,

203). Calcium release from endoplasmic reticulum occurs via inositol (1,4,5)-trisphosphate (IP₃)-induced Ca²⁺ release (IICR) and Ca²⁺-induced Ca²⁺ release (CICR) (Fig. 1).

Repetitive electrical stimulation of brain slices and slice cultures has been used to investigate transient elevations in [Ca²⁺]_m during synaptic activity. The major advantage of this experimental approach is that the resulting changes in synaptic activity affect a large population of neurons, thereby increasing the reliability of the fluorescence recording. Repetitive electrical stimulation for 10 s of the mossy fiber tract in hippocampal slice cultures elicited [Ca²⁺]_m transients that were characterized by an elevated plateau phase, compared with [Ca²⁺]_c transients during the stimulus train (102). Prolonged elevations in [Ca²⁺]_m for up to tens of seconds after train termination were only evident when neuronal activity was elicited in the upper physiological range (increases in [K⁺]_o of >2.5 mM), indicating slow mitochondrial Ca²⁺ extrusion. Increases in [Ca²⁺]_m showed strong positive correlation with stimulus intensity and frequency (5 to 100 Hz), as well as elevations in [K⁺]_o, suggesting a tight coupling of [Ca²⁺]_m transients and the degree of synaptic activity.

Similar data were reported for the hippocampal CA3 region of acute brain slices showing that brief electrical stimulus trains elicited transient elevations in [Ca²⁺]_m (17). However, in this study, the extracellular Mg²⁺ concentration was lowered to enhance excitability that led to spontaneous afterdischarges following the train and spreading waves in [Ca²⁺]_m. A more exact assessment of stimulus-induced transient Ca²⁺ elevations in dendritic mitochondria of hippocampal area CA3 was achieved by using analytical electron microscopy in hippocampal slice cultures (174). [Ca²⁺]_m was already significantly increased within 1 s after brief electrical stimulation (1 s, 50 Hz) and reached up to 10 times higher values at 30 s after stimulus, with a complete recovery after 180 s. At this time point [Ca²⁺]_c in the endoplasmic reticulum was still high, supporting the hypothesis that Ca²⁺ extruded from mitochondria might be taken up by intracellular stores. The difference between the two approaches might be explained by the fact that fluorescent Ca²⁺ probes measure free mitochondrial Ca²⁺ that is several orders of magnitude lower due to the high Ca²⁺ buffer capacity of the mitochondrial matrix, while analytical electron microscopy evaluates both free and bound Ca²⁺.

Elevations in [Ca²⁺]_m also occur in presynaptic structures during neuronal activation. Repetitive electrical stimulation of motor neurons (10–60 s, 50–100 Hz) resulted in an plateau elevation of [Ca²⁺]_m in mitochondria in axon terminals to about 1 μM (45), which is in the appropriate range for activation of mitochondrial dehydrogenases (145), but well below the value necessary for opening of the MPTP (230).

In addition to studies applying electrical stimulation, there is evidence that spontaneous neuronal activity also significantly affects [Ca²⁺]_m. Oscillations in [Ca²⁺]_m have been observed during spontaneous oscillatory changes in membrane potential and action potential firing of neurons in brain slices from the mouse respiratory center (150). The amplitude of these [Ca²⁺]_m oscillations correlated with the level of hypoxia that is the “physiological” stimulus for these cells. Moreover, changes in FAD and NAD(P)H fluorescence were also synchronized with [Ca²⁺]_m oscillations, indicating tight coupling of mitochondrial redox state and Ca²⁺ level (see below).

Electrical stimulation of brain slices results in activation of voltage-operated Ca²⁺ channels and NMDA receptor-gated channels leading to high local [Ca²⁺]_c domains. Whether elevations in [Ca²⁺]_m do also occur during activation of metabotropic receptors, as linked to the intracellular Ca²⁺ machinery, was explored in hippocampal slice cultures. Activation of metabotropic serotonergic, glutamatergic, and muscarinic receptors evoked transient elevations in [Ca²⁺]_m in a dose-dependent manner. Moreover, by isolating IICR, CICR, and receptor-operated capacitative Ca²⁺ entry, it was demonstrated that these individual pathways were able to transiently elevate [Ca²⁺]_m (103). These [Ca²⁺]_m transients were also immediately integrated in a metabolic response. Though applying microfluorometric techniques without any spatial resolution, the fluorescence was recorded in both stratum pyramidale, which contains densely packed neuronal cell bodies, and stratum radiatum. Thus the data suggest that neuronal mitochondria even sense elevations in [Ca²⁺]_c, as elicited by metabotropic receptor-mediated Ca²⁺ signaling (Fig. 1). This is in line with studies in individual neurons demonstrating that mitochondrial Ca²⁺ uptake buffers both IP₃-mediated and caffeine-induced [Ca²⁺]_c transients (123, 135).

The influence of the different Ca²⁺ sources on [Ca²⁺]_m is technically easier to assess in dissociated neuronal cultures. In this preparation, glutamate concentrations have been estimated to peak at 1.1 mM in synaptic clefts, with a decay time constant of 1.2 ms during neurotransmission (41). A likely source for mitochondrial Ca²⁺ uptake during synaptic activity is Ca²⁺ influx through NMDA receptor-gated channels. Activation of NMDA receptors (100 μM NMDA) in primary cultures of striatal neurons elicited similar and time-locked transients in [Ca²⁺]_c and [Ca²⁺]_m, whereas mitochondrial Ca²⁺ increases lagged behind cytosolic Ca²⁺ increases when the latter was induced by depolarization with high extracellular [K⁺] or by application of kainate or ionomycin (169). Comparably, NMDA and glutamate were most effective in filling mitochondrial Ca²⁺ stores in cultured cortical neurons, even at glutamate concentration as low as 3 μM (22). Application of 20 μM and 200 μM NMDA to cultured hippocampal neurons resulted in a rise in [Ca²⁺]_c and [Ca²⁺]_m, as revealed by the chemiluminescence change of mitochondrially targeted aequorin (219). Interestingly, only application at 200 μM enhanced Ca²⁺ cycling across the inner membrane, which might explain the increased neurotoxicity at this concentration. Thus, it seems that neuronal mitochondria take up Ca²⁺ from different sources during synaptic activity. However, individual mitochondria may prefer a particular Ca²⁺ source based on the location in the cytosol (11, 45, 175).

Heterogeneity of [Ca²⁺]_m in Neuronal Mitochondria

Ca²⁺ signaling in neurons is characterized by complex spatiotemporal patterns (4, 10). Mitochondria that are equipped with effective Ca²⁺ transport mechanisms and that are located at important strategic points in dendrites and presynaptic segments might contribute to this spatiotemporal complexity (16, 174, 185, 196, 223). Changes in [Ca²⁺]_m of individual mitochondria have been monitored in hippocampal slice cultures by applying high-resolution confocal laser-scanning microscopy and offline spatial frequency filtering methods (112). [Ca²⁺]_m was highly heterogeneous between individual mitochondria,

even under resting conditions without any external stimulation. This heterogeneity was present in each slice culture irrespective of the staining method (via patch pipette or bulk loading of slices) or the K_d of the rhod-dye derivative used (0.5 μM and 19 μM). Interestingly, mitochondria with a granular appearance expressed brighter fluorescence, indicating elevated basal levels in $[\text{Ca}^{2+}]_m$, whereas the fluorescence was rather low in filamentous mitochondria. Colocalizing MitoTracker Green and rhod-2 fluorescence identified mitochondrial filaments that contained rhod-2 fluorescence hot spots of granular appearance, suggestive for high local Ca^{2+} domains in mitochondria. This might indicate that either mitochondrial filaments are spatially discontinuous or diffusion barriers for Ca^{2+} exist within mitochondrial filaments. A recent study on rat brain capillary endothelial cells demonstrated that the extension of mitochondria differs in terms of electrical continuity and distribution of $[\text{Ca}^{2+}]_m$. It was concluded that diffusion of Ca^{2+} is limited to a single mitochondrion, whereas changes in $\Delta\Psi_m$ might spread over mitochondria forming an electrically continuous syncytium (71). If this mechanism is also present in neurons, it would allow restriction of elevations in $[\text{Ca}^{2+}]_m$ and thus activation of TCA dehydrogenases in the locations of high $[\text{Ca}^{2+}]_c$ domains, whereas the cost of mitochondrial Ca^{2+} uptake, namely mitochondrial membrane depolarization, would be distributed over the mitochondrial network. Thus ATP formation might be optimally enhanced at the place of highest demand (202).

Additionally, ultrastructural and confocal laser-scanning microscope studies suggest that the distribution of the mitochondrial population in neurons and glial cells is largely heterogeneous and dynamically changing (44, 49, 149, 177). Mitochondrial filaments were found in vivo in the soma, dendrites, and axons of principal cells in dentate gyrus and areas CA1 and CA3 of the hippocampus. Interestingly, mitochondria do not seem to invade spines with the exceptions of the thorny excrescences in CA3 (177). This observation slightly differs from those made in vitro. This is possibly due to the fact that formation of such filaments from smaller granular mitochondria is a dynamic process (23, 49, 149). Mitochondria may undergo continuous fusion and fission cycles (37, 225), thus building up larger entities serving for more effective distribution of proton motive force (202). However, a balance shift toward the granular form (thread-grain transition) might be also an early sign of cell damage and apoptosis (201). Continuous fusion and fission cycles might also explain the recovery of the chemiluminescence of mitochondria-targeted aequorin during repetitive NMDA application to hippocampal neurons (11). It is possible that the aequorin pool, which is consumed during the first NMDA application in mitochondria closely situated to the plasma membrane, is replenished by mitochondrial transport and/or fusion with mitochondria from the bulk cytosol. In contrast to dendrites and somata, mitochondria in the axons and in presynaptic endings are rather granular in shape, which might influence their capability to act as a local Ca^{2+} buffer (177, 196).

Another aspect of mitochondrial Ca^{2+} buffering is related to the fact that mitochondria are highly motile organelles showing anterograde and retrograde transport in dendrites and axons, as well as small Brownian "wiggling" (149, 163). The velocity of the directed movements in neurons was largely dependent on temperature, with values about 0.36 $\mu\text{m/s}$ (112), 0.6 $\mu\text{m/s}$ (50),

and 0.32–0.38 $\mu\text{m/s}$ (153). Directed transport along microtubules is mediated by the dynein-kinesin system, whereas mitochondria also move along actin filaments by using myosin motors (88). Mitochondrial transport was shown to be influenced by Ca^{2+} because local elevations in $[\text{Ca}^{2+}]_c$ led to an immediate stop of mitochondrial movement (182). This mechanism might enhance mitochondrial Ca^{2+} uptake by retaining mitochondria at places of Ca^{2+} release/influx and serve for energy supply in response to local demands (226).

Synaptosomal and somatic mitochondrial fractions show different sensitivities to excessive Ca^{2+} challenge because synaptosomal mitochondria, which are primarily presynaptic, more rapidly undergo MPTP opening (27). Since axonal transport often implies long distances, axonal and presynaptic mitochondria might represent an aged group in the mitochondrial population. Indeed, monitoring $\Delta\Psi_m$ showed that highly polarized mitochondria were transported in the anterograde direction while partially depolarized mitochondria were transported retrogradely along the axon (148).

Involvement of Mitochondrial Ca^{2+} Signaling in Neuronal Behavior

Mitochondrial dysfunction and particularly mitochondrial ROS formation in the CNS is involved in acute insults like ischemia-reperfusion injury and in chronic neurodegenerative disorders like Alzheimer and Parkinson disease (39, 162). Much less is known on mitochondrial interactions with neuronal behavior under physiological conditions. Changes in $[\text{Ca}^{2+}]_c$ play a critical role in neuronal development, neurotransmitter release, and plasticity. In the previous section we discussed the tight coupling between cytosolic and mitochondrial Ca^{2+} signals, and there is accumulating evidence that changes in $[\text{Ca}^{2+}]_m$ serve as a regulatory mechanism for adaptation of mitochondrial energy metabolism when neuronal activity is in the physiological range (see below).

Mitochondrial Ca^{2+} uptake shapes the spatiotemporal pattern of cytosolic Ca^{2+} signals and may thus influence neuronal behavior. It has been shown that mitochondrial Ca^{2+} buffering decreases the peak amplitude of stimulus-induced $[\text{Ca}^{2+}]_c$ transients and slows $[\text{Ca}^{2+}]_c$ recovery by slowly recycling Ca^{2+} into the cytosol (22, 42, 43, 68, 169, 219–221). By shaping the time course of $[\text{Ca}^{2+}]_c$ transients in neurons, mitochondria can exert control on processes that are dependent on the perfect timing and localization of Ca^{2+} gradients, like release of synaptic vesicles. $[\text{Ca}^{2+}]_c$ elevation and subsequent synaptic transmission, as induced by high-frequency stimulation, seemed to be regulated by mitochondrial Ca^{2+} uptake in motor neuron terminals (46, 70) and at the retinal amacrine cell synapse (146). Nevertheless, a recent study in a *Drosophila* mutant lacking mitochondria in synapses suggests that mobilizing the reserve pool of synaptic vesicles depends on the presence of ATP rather than on mitochondrial Ca^{2+} buffering (214).

Mitochondria may also contribute to certain forms of synaptic plasticity. The phenomenon of post-tetanic potentiation is characterized by an increase in synaptic strength after high-frequency stimulation. The underlying mechanism is a short-term increase in synaptic release probability due to residual Ca^{2+} in the presynaptic terminal following strong stimuli (51). This form of short-term synaptic plasticity can be also ob-

served at the neuromuscular junction. It was demonstrated that blocking mitochondrial, but not endoplasmic reticulum Ca^{2+} uptake, prevented posttetanic potentiation. Mitochondrial Ca^{2+} buffering kept $[\text{Ca}^{2+}]_c$ below $1 \mu\text{M}$ during a tetanus, whereas the recovery of $[\text{Ca}^{2+}]_c$ was largely prolonged due to subsequent extrusion of Ca^{2+} from the mitochondria, resulting in an increase of synaptic release probability in this period (210).

The high-frequency stimulation in the previous examples results in high $[\text{Ca}^{2+}]_c$ transients, and it is commonly accepted that mitochondrial Ca^{2+} uptake is activated at such levels (174, 220). However, there is also evidence that mitochondria contribute to presynaptic Ca^{2+} buffering, even after a brief stimulus train (4 pulses, 100 Hz) at the glutamatergic synapse of the calyx of Held. In this preparation, mitochondrial Ca^{2+} -buffering determined the fast recovery of postsynaptic currents after stimulus-induced synaptic depression (16).

In contrast, at the ribbon synapse of the retinal bipolar neurons, the plasma membrane Ca^{2+} pumps were responsible for the Ca^{2+} removal from the cytosol, and mitochondrial Ca^{2+} uptake was observed only in about 30% of the cells. Concomitantly, mitochondrial ATP delivery was inevitable for proper functioning of the plasma membrane Ca^{2+} pumps, suggesting involvement of presynaptic mitochondria in synaptic transmission (227). The difference between these two types of synapses might be the localization of mitochondria with respect to Ca^{2+} entry sites (223).

Based on these examples it might be concluded that the general mechanisms of mitochondrial contribution to synaptic transmission are shaping of the spatiotemporal pattern of cytosolic Ca^{2+} signals and accurate ATP delivery for restoration of ion gradients and vesicle pool cycling. However, the extent to which a certain mechanism influences neuronal behavior has to be determined for each type of synapse.

Another important consequence of Ca^{2+} uptake is mitochondrial ROS formation, which has been shown for neuronal preparations in studies on excitotoxicity (18, 33, 57, 181). However, there is also evidence that endogenous glutamate release under physiological conditions leads to moderate increases in ROS formation, which modulates intracellular signaling cascades (89), synaptic transmission (7), as well as communication between neurons and glial cells (5).

Changes in $\Delta\Psi_m$ During Physiological Synaptic Activity

The driving force for mitochondrial Ca^{2+} uptake is mainly represented by the mitochondrial membrane potential. Since both the Ca^{2+} uptake and extrusion mechanisms are electrogenic (Refs. 12, 75, 98; but see Ref. 20), elevations in $[\text{Ca}^{2+}]_m$ associated with synaptic activity might result in a decrease in $\Delta\Psi_m$. In addition, several factors like substrates, free radicals, and changes in ATP/ADP ratio might significantly influence $\Delta\Psi_m$ during synaptic activity.

The same stimulation protocols, which were shown to elicit a $[\text{Ca}^{2+}]_m$ transient or even a spreading wave of $[\text{Ca}^{2+}]_m$, were also effective to evoke a spreading wave of mitochondrial depolarization in hippocampal slices (17). The fact that the amplitude of mitochondrial depolarization correlated with the intensity of synaptic activity and that $\Delta\Psi_m$ changes spread along anatomical pathways and were blocked by inhibition of the voltage-operated Na^+ channels or glutamatergic transmission, strongly indicate the dependence of changes in $\Delta\Psi_m$ on

synaptic activity. The spatiotemporal pattern of changes in $\Delta\Psi_m$ correlated with that of the stimulus-induced $[\text{Ca}^{2+}]_m$ under the same experimental paradigm, suggesting that changes in mitochondrial Ca^{2+} cycle might underlie the depolarization of mitochondrial membranes. In line with these findings, spontaneous oscillations in $[\text{Ca}^{2+}]_m$ in neurons of the respiratory center were associated with time-locked oscillations in $\Delta\Psi_m$ (150). It is noteworthy, however, that differences in $\Delta\Psi_m$ might be influenced by factors other than the regional differences in synaptic activity. It has been shown that mitochondria isolated from the CA1 region are more susceptible to an excessive Ca^{2+} load than mitochondria from the CA3 region (143). There might be also age-dependent differences in the ability of mitochondria to cope with such a Ca^{2+} load. Both mitochondrial Ca^{2+} buffering capacity and $\Delta\Psi_m$ were decreased in forebrain neurons from aged rats (155). In line with these findings, recovery of $\Delta\Psi_m$ was slowed down in cerebellar brain slices from old rats after depolarization with a high extracellular K^+ concentration, suggesting increased vulnerability of aged mitochondria (224). The Ca^{2+} dependence of the $\Delta\Psi_m$ was also shown in individual patched CA1 pyramidal cells in acute hippocampal slices (191). Depolarization steps resulted in a $[\text{Ca}^{2+}]_c$ transient and a delayed loss in $\Delta\Psi_m$. This loss in $\Delta\Psi_m$ was dependent on Ca^{2+} influx through voltage-operated Ca^{2+} channels because it was suppressed in zero Ca^{2+} ACSF.

In these studies strong stimuli were applied, which likely evoked neuronal activity above the physiological range. Nevertheless, we have also observed mitochondrial depolarization when applying moderate electrical stimulation or the muscarinic receptor agonist carbachol in slice cultures (Kann and Kovács, unpublished observation).

However, even this type of physiological stimulation results in neuronal activity, which is different from the activity which mitochondria might experience during spontaneous synaptic activity in slices. When using laser-scanning confocal microscopy for monitoring $\Delta\Psi_m$ in patched pyramidal cells, a considerable heterogeneity in rhodamine 123 fluorescence was observed. Filamentous mitochondria expressed rather low fluorescence compared with granular mitochondria and mitochondrial clusters (112). This is in line with findings from neuronal cultures showing mitochondrial differences in form and polarization by using the ratiometric mitochondrial probe JC-1 (49, 163). Despite the high level of background synaptic activity, spontaneous fluctuations in $\Delta\Psi_m$ were rarely observed in normal ACSF. However, Ca^{2+} buffering via the patch pipette solution (1 mM EGTA) might have masked physiological, small-amplitude changes in $[\text{Ca}^{2+}]_c$, finally suppressing fluctuations in $\Delta\Psi_m$ (112).

Spontaneous fluctuations in $\Delta\Psi_m$ have been observed in neuroblastoma cells and in primary neuronal cultures (29, 136). Interestingly, these fluctuations were not dependent on synaptic activity because they persisted in the presence of tetrodotoxin (TTX) and the NMDA receptor blocker MK-801. Although they were also resistant to cyclosporin A, the contribution of MPTP to the $\Delta\Psi_m$ fluctuations cannot be completely excluded because cyclosporin A did not block Ca^{2+} -induced MPTP-opening in the presence of ATP in nonsynaptic brain mitochondria (28, 40). Alternatively, this phenomenon might represent changes in oxidative phosphorylation (81) or changes in electrogenic channel or transporter activity of the mitochon-

drial membrane. Indeed, prolonged multiple openings of mitochondrial ion channels have been observed in the presynaptic terminal of the squid giant presynaptic terminal during stimulus-induced synaptic transmission (95, 96).

In conclusion, these data suggest that even moderate changes in $\Delta\Psi_m$ can be induced by a broad spectrum of physiological stimuli. The underlying mechanisms may differ depending on the type of stimulus as well as on the preparation used. However, a close interplay between Ca^{2+} cycling across the inner membrane and mitochondrial depolarization is proposed.

Since mild loss of $\Delta\Psi_m$ has been proposed to decrease mitochondrial ROS formation (165), there is an apparent contradiction between the Ca^{2+} -dependent increase in ROS formation, which we described in the previous section, and the Ca^{2+} -dependent decrease in $\Delta\Psi_m$. Indeed, mitochondrial ROS formation at its major sites, namely, complex III and complex I, was shown to be decreased or completely inhibited by depolarization of the mitochondrial membrane (158, 206, 216). In line with these findings, a neuroprotective role has been proposed for the mitochondrial uncoupling proteins (UCPs), the expression of which is upregulated after insults to the CNS (108). One alternative source of $\Delta\Psi_m$ -independent superoxide radical formation might be α -ketoglutarate dehydrogenase, which might also explain the upregulation of ROS formation in the presence of high $[\text{Ca}^{2+}]_m$ and NADH (39, 205). Moreover, once undergoing autoxidation, complex I can produce ROS in a vicious cycle, irrespective of $\Delta\Psi_m$ (117). In conclusion, Ca^{2+} -dependent, mild mitochondrial depolarization might exert an inhibitory effect on ROS formation that, however, might be surpassed by other targets of the Ca^{2+} load.

NAD(P)H and FAD Transients

Changes in NAD(P)H fluorescence have been used to monitor adaptations in energy metabolism during neuronal activity in brain slice preparations (133, 190). Stimulus-evoked neuronal activity results in characteristic biphasic NAD(P)H fluorescence transients, namely, a brief initial “dip” component and a subsequent prolonged “overshoot” component. Such NAD(P)H transients can be elicited by repetitive electrical stimulation or application of receptor agonists (102, 103, 197). The typical time course of NAD(P)H transients is in the range of 3–4 min when a stimulus train of 10 s is applied at 20 Hz. Changes in Po_2 , as well as application of substrates and drugs interfering with mitochondrial targets and metabolism, elicit slower baseline shifts in NAD(P)H fluorescence (65, 102, 133).

Characteristics of tissue and cellular levels. The ratio between “dip” and “overshoot” components varies between the cellular and tissue levels in the brain. In the early in vivo studies, NAD(P)H fluorescence transients primarily consisted of large “dip” components in the cerebral cortex upon direct electrical stimulation, evoked seizures, or spreading depression (97, 144, 184). Though the in vivo approach allowed optimal oxygen supply to the brain parenchyma, these studies were restricted to the cortical surface, thus reflecting changes in NAD(P)H fluorescence of apical dendrites and meninges. In brain slices, it was found that NAD(P)H transients almost exclusively displayed a “dip” component upon electrical stimulation or local glutamate application in the alveus (a hippocampal structure that predominantly contains neuronal fiber

tracts), while biphasic NAD(P)H transients with an accentuated overshoot component occurred in *s. radiatum* (containing synapses, neuronal fiber tracts, and glial cells) (197). Therefore, the shape of NAD(P)H transients seems to depend on a variety of factors that include tissue Po_2 levels, the ratio between neurons (neuronal segments) and astrocytes, as well as cellular biochemical properties. Interestingly, applying high-resolution, two-photon laser-scanning microscopy in acute hippocampal slices, it was reported that stimulus-evoked dip and overshoot components of NAD(P)H transients were highly anti-colocalized in *s. radiatum*. Moreover, it was proposed that the dip represented a neuronal response, whereas the overshoot was primarily astrocytic, indicating a compartmentalization of oxidative and glycolytic metabolism between neurons and astrocytes (105). These findings may argue for the astrocyte-neuron lactate shuttle hypothesis (139). Nevertheless, biphasic NAD(P)H transients were described in individual sensory, hippocampal, and cerebellar neurons of dissociated cell cultures (56, 83, 193), similar to other excitable and nonexcitable cells (79, 178, 222). Moreover, biphasic NAD(P)H transients have recently been found to be unaffected by inhibition of glycolysis, as well as glucose uptake blockade, over a wide range of electrical stimulation in acute hippocampal slices (21). These experiments were conducted under conditions with provision of pyruvate as an alternative substrate and when adenosine-1 receptor antagonists prevented decreases in synaptic efficacy. The findings suggest that NAD(P)H transients reflect mitochondrial rather than glycolytic processes.

Ca²⁺-dependent and -independent NAD(P)H transients. Adaptation of local energy demands in neurons requires intracellular signals integrating neuronal activity and metabolic responses of mitochondria. One likely candidate is intracellular Ca^{2+} because 1) activated neurons experience transient intracellular Ca^{2+} loads up to the micromolar range, and 2) the activity of TCA cycle enzymes, for example, is stimulated by Ca^{2+} elevations (80, 145).

The tight temporal association between transient elevations in cytosolic and mitochondrial Ca^{2+} concentrations and NAD(P)H (and FAD) fluorescence transients during neuronal activity has been shown in brain slice preparations (102, 103, 150, 197), which is supported by studies in dissociated neuronal cultures (56, 193). Moreover, significant reductions in the amplitude of NAD(P)H transients during electrical neuronal stimulation and under experimental conditions that prevent intracellular and mitochondrial Ca^{2+} elevations, strongly support the hypothesis that Ca^{2+} is a key integrator for neuronal activity and mitochondrial energy metabolism (56, 102). Nevertheless, a significant portion of NAD(P)H transients seems to be Ca^{2+} independent in slice preparations (102, 197), similar to FAD transients in the in vivo cerebellum (180). The underlying mechanisms have not been clearly defined and are still under discussion. However, this finding has been particularly observed during prolonged neuronal stimulation that is per se associated with activity-dependent transient increases in $[\text{K}^+]_o$ (102), as well as under a condition where neurotransmitter release was not inhibited (197). Both factors may trigger Ca^{2+} -independent pre- and postsynaptic neuronal as well as astrocytic mechanisms, which include glutamate uptake and metabolism and/or activation of ATPases (for discussions see Refs. 21, 102, 105, 132).

In summary, the available data based on NAD(P)H and FAD fluorescence studies point to a complex regulation of energy metabolism in brain tissue. It is conceivable that mitochondrial Ca^{2+} accumulation as a local “extrinsic” signal adapts oxidative metabolism in mitochondria, which gets superimposed on an “intrinsic” regulation of NADH redox states (145). Candidates for such intrinsic regulation are the ratios of ADP/ATP, NAD^+/NADH , or CoA/acetyl-CoA (80, 99, 145). This might suggest an indication of coming metabolic demand for neuronal mitochondria that is mediated by Ca^{2+} , as well as a feedback control that is ultimately mediated by ATP consumption.

Fine-tuned neurometabolic coupling. Some of the studies discussed above also provide clear evidence that neuronal activity and mitochondrial function are tightly coupled in neurons. Positive quantitative correlations between gradual neuronal activity, transient elevations in $[\text{Ca}^{2+}]_c$ and $[\text{Ca}^{2+}]_m$, as well as amplitudes of NAD(P)H transients, have been demonstrated when the parameters of electrical stimulation (intensity, frequency, or duration) or concentrations of applied neurotransmitters and drugs were gradually increased (56, 102, 103, 125, 197). Interestingly, clear positive correlations persisted over the whole range of physiological stimulation (monitored by transient increases in $[\text{K}^+]_o$ from 0.25 to 3 mM), indicating a tight coupling between neuronal activity and mitochondrial metabolic responses. These relations seemed to uncouple only under conditions of extended neuronal activity with short time intervals between stimulus trains and when the NAD(P)H “overshoot” had not yet recovered to baseline (102). This might be explained by ceiling levels of NAD(P)H fluorescence, possibly because of maximal reduction of the available nicotinamide adenine dinucleotides pool in the tissue.

From the studies discussed, there is also clear evidence for tight temporal relations between neuronal activity and mitochondrial function in brain slices. Almost immediately with onset of repetitive stimulation and rapid increases in $[\text{Ca}^{2+}]_c$ and $[\text{Ca}^{2+}]_m$, NAD(P)H fluorescence starts to decrease while the nadir of the resulting “dip” component is reached during or at termination of the stimulus train, depending on the stimulus parameters. This is in line with data demonstrating rapid Ca^{2+} -dependent mitochondrial NAD(P)H oxidation and O_2 consumption that occurs within 0.2 s after onset of depolarization of cerebellar Purkinje neurons (83).

These tight quantitative and temporal relations between neuronal activity and mitochondrial function point to a fine-tuned “neurometabolic coupling” in the brain, which preserves neuronal excitability and neurotransmission in the acute phase during activation and as long as substrates are supplied to the parenchyma. In brain slice preparations, this prerequisite may be considerably masked due to the high concentrations of glucose in ACSF and/or the limiting prolonged diffusion distances for O_2 . However, in the *in vivo* brain sufficient substrate supply to the parenchyma is achieved by a highly developed network of vessels and capillaries with distances of 20–40 μm and a variety of complex regulatory mechanisms that may be attributed to the processes of “neurovascular coupling” and “neurobarrier coupling.” Neurovascular coupling designates the adaptation of blood vessel diameter and thus blood flow to the degree of neuronal activity (87, 215). The increase in regional blood flow matches the local needs of brain cells for nutrients after neuronal activation. This process requires func-

tional links between neurons, astrocytes, and vascular cells that may form neurovascular units. Possible signaling factors are NO, adenosine, arachidonic acid metabolites, and elevations in $[\text{K}^+]_o$ (32, 53, 160, 229). Neurobarrier coupling designates adaptations in the properties of glucose transport across the blood-brain barrier after neuronal activation, which may include changes in Michaelis-Menten parameters of the GLUT-1 protein, activity-dependent incorporation of GLUT-1 in blood-brain barrier membranes, and/or changes in GLUT-1 expression in response to chronic (developmental or pathological) changes in neuronal activity and/or plasma glucose concentrations (126). Neurovascular coupling is evident on the order of seconds after neuronal activation (140), while neurobarrier coupling may also imply long-term changes of at least hours or days at the blood-brain barrier. Thus both processes overlap in part with and follow up on neurometabolic coupling to synergistically fulfill the energy demands of neurons.

MITOCHONDRIAL DYSFUNCTION AND TEMPORAL LOBE EPILEPSY

Temporal Lobe Epilepsy and Experimental Models

Epilepsy is one of the most common acquired chronic neurological diseases that affects about 0.8% of the human population (82). Although treated with antiepileptic drugs, about 50% of epilepsy patients still experience seizures. Temporal lobe epilepsy (TLE) is a prevalent form of focal epilepsy, which is frequently resistant to drugs. In some patients TLE might be a progressive disease (172). A selected group of drug-resistant TLE patients benefits from surgical resection of the epileptogenic focus in the temporal lobe and hippocampus (59). In histopathology, hippocampal tissue from TLE patients is often characterized by neuronal cell loss and astrogliosis (141). Other studies have described reorganization of neuronal networks (208) and functional alterations of receptors and ion channels (6), which might explain neuronal hyperexcitability and hypersynchrony in epileptogenic tissue. Nevertheless, the mechanisms underlying the pathogenesis of TLE are still unclear. In the initial phase of seizure activity, cerebral blood flow drastically increases up to 400–900% of control values, depending on the brain region (93, 147), which matches the increase in amplitude of local metabolic rates for glucose. After 1–2 h of recurrent seizures or status epilepticus, local cerebral blood flow decreases to 150–300%. This results in a relative hypoperfusion, while the metabolic demand remains high due to ongoing seizure activity. Based on these facts it has been suggested that the maladjustment between blood supply and energy metabolism plays a central role in seizure-induced neuronal cell death (93, 116, 209). Nevertheless, pathological neuronal activity might also induce mitochondrial dysfunction and ROS production in the early phase of seizure activity, which finally contributes to neuronal cell death (13). Moreover, functional neuroimaging studies in the interictal phase of epilepsy patients demonstrated a decrease in glucose utilization in seizure foci and adjacent brain structures (34, 118). Such chronic “hypometabolism” might be explained by dysfunction of mitochondrial oxidative and/or glycolytic energy metabolism.

Below, we will summarize evidence for acute and chronic alterations of mitochondrial function and energy metabolism as derived from experimental models of TLE. Studies on mito-

chondrial function during epileptic processes have been conducted by applying primarily two experimental approaches. In the first approach, epileptiform activity is pharmacologically elicited in brain slice preparations from healthy animals. In the second approach, brain slices are made from animal models of TLE. In pilocarpine-treated, chronic epileptic rats, for example, symptoms, histopathology, and course of the disease resemble those occurring in TLE patients (35, 141).

Changes in $\Delta\Psi_m$ and $[Ca^{2+}]_m$ During Epileptiform Activity

As discussed above, there is evidence that $\Delta\Psi_m$ and $[Ca^{2+}]_m$ are influenced to a certain degree by stimulus-induced synaptic activity in brain tissue. Epileptiform activity, as induced in the low- Mg^{2+} model in vitro, can be classified by interictal events, seizure-like events (SLEs), and late recurrent discharges, the latter of which is insensitive to antiepileptic drugs (115). Interictal activity did not cause detectable changes in $[Ca^{2+}]_c$, $[Ca^{2+}]_m$, and $\Delta\Psi_m$ at the tissue level, when studied with microfluorometric recordings in slice cultures. In contrast, SLEs elicited large $[Ca^{2+}]_c$ transients that were associated with elevations in $[Ca^{2+}]_m$ and loss in $\Delta\Psi_m$. The recovery of both $[Ca^{2+}]_m$ and $\Delta\Psi_m$ to values before SLEs outlasted synchronized neuronal activity by several minutes, a process that might acutely compromise energy metabolism (113, 114). When applying high-resolution confocal microscopy, small-amplitude fluctuations in $[Ca^{2+}]_m$ and $\Delta\Psi_m$ were associated with interictal activity and never did occur during control conditions in normal ACSF (112). However, it was hard to find a correlation between brief interictal discharges (~ 1 s, 0.2 to 0.7 Hz) and fluctuations in $[Ca^{2+}]_m$ and $\Delta\Psi_m$ that lasted for up to 20 s. Fluctuation in $\Delta\Psi_m$ occurred primarily in the dendrites but not in the soma. A possible explanation is that local Ca^{2+} changes due to enhanced NMDA receptor activity and/or dendritic voltage-dependent Ca^{2+} conductance are sensed locally by few mitochondria, whereas the distance to somatic mitochondria is too far from the Ca^{2+} influx sites during interictal activity. By contrast, during SLEs a massive and synchronous loss in $\Delta\Psi_m$ occurred in neuronal dendrites and somata. Interestingly, amplitude and frequency of $[Ca^{2+}]_m$ fluctuations increased significantly on the level of individual mitochondria during SLEs while baseline $[Ca^{2+}]_m$ did not increase, indicating no net Ca^{2+} accumulation. However, averaging rhod-2 fluorescence in a large population of mitochondria at a given time point revealed elevation in $[Ca^{2+}]_m$ similar to microfluorometric data from the tissue level. SLE-associated $[Ca^{2+}]_m$ but not $[Ca^{2+}]_c$ fluctuations were inhibited in the presence of Ru360 in the perfusion (112), indicating specific block of the Ca^{2+} uniporter by Ru360 (see also Ref. 142). Intracellular application of either Ru360 or the mitochondrial Na^+/Ca^{2+} exchanger blocker CGP-37157 via the patch pipette also prevented synchronized loss of $\Delta\Psi_m$, whereas cyclosporin A, an inhibitor of MPTP opening, had no effect when added to the perfusion (112). Though there is the possibility of cyclosporin A-resistant MPTP openings (28, 40), the fact that the selective block of the Na^+/Ca^{2+} exchanger alone was sufficient to prevent changes in $\Delta\Psi_m$ indicates that enhanced mitochondrial Ca^{2+} cycling across the inner membrane might dissipate $\Delta\Psi_m$ in a futile cycle. Lasting $\Delta\Psi_m$ dissipation might explain the decrease in ATP production as seen during seizures in vivo (64, 77), which might contribute to neuronal cell death. Thus the

same mechanism by which synaptic activity regulates energy metabolism under physiological conditions might be responsible for the acute devastating effects of seizure activity on $\Delta\Psi_m$ (Fig. 2).

Mitochondrial ROS Formation During Epileptiform Activity

One possible consequence of enhanced mitochondrial Ca^{2+} cycling might be an increase in production of ROS (Figs. 1 and 2). ROS formation was enhanced in isolated mitochondria exposed to elevated extramitochondrial $[Ca^{2+}]$ and $[Na^+]$ (58), mimicking conditions that might occur during seizures. There is substantial indirect evidence for involvement of ROS in the seizure-induced cell loss from a variety of in vivo models of epilepsy that include fluorothyl-induced seizures (63), the kindling model of epilepsy (67), as well as the pilocarpine and kainic acid model of epilepsy (168, 170). Oxidative damage of mitochondrial enzymes has been found in chronic epileptic tissue from animal models (120, 131) and in resected human tissue (119). ROS formation is not only a consequence of sustained epileptic activity. ROS might also be a cause of epileptic activity because moderate oxidative stress in mitochondrial superoxide dismutase (SOD2) +/- mice has been attributed to spontaneously occurring seizures (130).

Mitochondrial ROS formation during epileptiform activity has been also demonstrated in hippocampal slice cultures using fluorescence indicators (66, 113). Based on the relative specificity of the chosen fluorescent probes (18), superoxide radical was the most likely formed ROS in these experiments. Other ROS like hydroxyl, alkyl, and peroxy radicals, formed in subsequent reactions, might also contribute to neuronal injury (213). This is supported by the neuroprotective effects of the free radical scavenger α -tocopherol, which is a lipid peroxidation chain breaker, as well as by the observation of increased levels in the lipid peroxidation end-product malondialdehyde in epileptic tissue (66, 67, 113). While a decrease in the

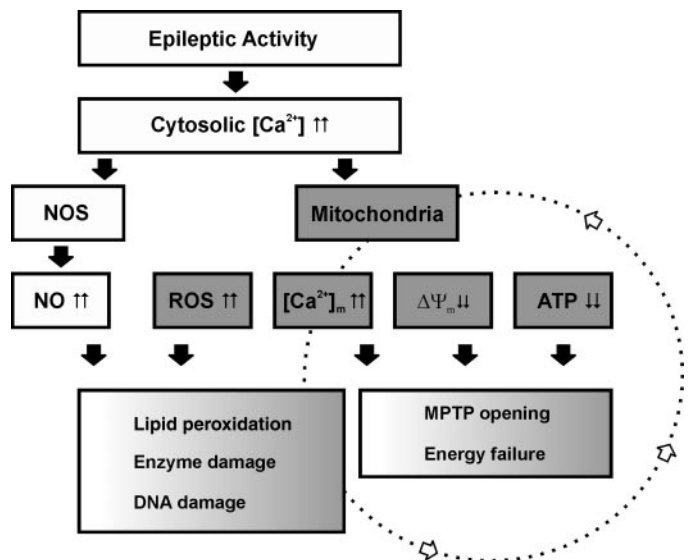


Fig. 2. Scheme illustrating the pathological mechanisms in cytoplasm (light gray) and mitochondria (dark gray), as well as their consequences that might contribute to neuronal cell injury and death in temporal lobe epilepsy. Cellular and mitochondrial DNA and/or enzyme damage might enhance mitochondrial vulnerability in a vicious cycle (dotted circle). NO (nitric oxide), NOS (NO synthase).

mitochondrial content of the intrinsic antioxidant glutathione was demonstrated after kainic acid-induced seizures in vivo (129), the elevation of glutathione levels was neuroprotective in vitro and in vivo (66, 67).

NO is another free radical that might contribute to alterations in energy metabolism and neuronal injury during seizures. Studies applying electron spin resonance spectroscopy have demonstrated elevated NO levels after seizures in vivo, as induced by kainic acid (106) and pentylentetrazole (100). Moreover, elevated levels of citrulline, the byproduct of NO synthesis, have been determined after acetylcholinesterase inhibitor-induced status epilepticus (77). Activation of NMDA receptors has been related to enhanced NO formation (31, 107), which is of particular importance for the low-Mg²⁺ model of epilepsy (152). Indeed, increased NO formation occurs during epileptiform activity in entorhinal cortex slices in this model, and NO synthase inhibition blocked epileptiform activity (189). This indicates a regulatory role for NO in the initiation of SLE by a hitherto unknown mechanism. The existence of a mitochondrial NO synthase is still controversial (Refs. 73, 212; but see Ref. 122). Nevertheless, this issue is very important because NO has been reported to block oxidative respiration, reversibly and irreversibly (25, 186). Thus, extensive NO formation might significantly disturb energy metabolism during epileptiform activity. Another study reported that neuronal tissue tolerates high NO levels (107). Nevertheless, in the presence of superoxide radical, NO forms highly reactive peroxynitrite, which might induce oxidative damage of mitochondrial and cellular structures like membranes and DNA. Degradation of the mitochondrial phospholipid cardiolipin leads to irreversible inhibition of the respiratory chain, whereas extensive DNA damage activates the nuclear protein poly-(ADP-ribose) polymerase (PARP), resulting in depletion of cytosolic NAD and inhibition of glycolysis. Glycolysis is also inhibited due to the direct oxidation of glyceraldehyde-3-phosphate dehydrogenase by peroxynitrite. Thus NO and peroxynitrite may cause necrosis via ATP depletion. In addition, peroxynitrite, S-nitrosothiols, NO₂, and/or N₂O₃ may cause neuronal apoptosis by directly activating MPTP, leading to cytochrome *c* release and caspase activation during seizures (13, 48, 168) (Fig. 2).

Metabolic Dysfunction During Epileptiform Activity

When pathological epileptiform activity was elicited in the low-Mg²⁺ model in hippocampal slice cultures and acute slices of the entorhinal-hippocampal cortex, SLEs initially induced robust biphasic NAD(P)H transients similar to conditions with physiological stimulation. Nevertheless, with the increase in number of SLEs, severe alterations in NAD(P)H transients occurred, namely, a decrease and finally a complete loss of the overshoot component (113, 192). These alterations in NAD(P)H transients may reflect mitochondrial dysfunction that causes acute energy failure, probably as a consequence of the massive ROS production during SLEs. However, these findings have to be proved in other acute experimental models of epilepsy before final conclusions can be made.

Interestingly, similar alterations were observed when NAD(P)H transients, as elicited by electrical stimulation, were investigated in hippocampal slices from chronic epileptic rats and resected brain tissue of TLE patients (101). NAD(P)H

transients showed smaller overshoot components in area CA1 compared with the subiculum in chronic epileptic rats, indicating region-specific alterations. In hippocampal tissue from TLE patients, NAD(P)H fluorescence transients showed marked initial "dip" components and lacked an overshoot component in most of the cases. These findings indicate severe mitochondrial and metabolic dysfunction in tissue from chronic epileptic rats and humans. In TLE patients, the dysfunction might be more pronounced because of seizure history over years or even decades. Similar alterations in stimulus-induced NAD(P)H fluorescence transients were also observed in hippocampal slices from kainate-treated, chronic epileptic rats (120). These studies from animal models and pathological human brain specimens provide evidence for a cellular correlate for hypometabolism, as observed in neuroimaging studies in epilepsy patients. The underlying mechanisms are still under discussion and include defects in mitochondrial enzymes like complex I and aconitase (119, 131), dysfunction of neuronal-astrocytic metabolic coupling (139), and/or abnormal Ca²⁺ cycling (120).

CONCLUSIONS AND PERSPECTIVES

Mitochondria in neurons form a compartment that is highly dynamic in structure and function. This involves mitochondrial transport in neuronal segments and strategic positioning of mitochondria at sites where ATP supply and Ca²⁺ handling is required. Moreover, a fine-tuned coupling between neuronal activity and mitochondrial function exists that is mediated by ions and substrates. Thus, mitochondria are critically involved in neuronal survival, neurotransmission, and plasticity. New high-resolution imaging techniques will help to extend our knowledge on the physiological interactions between neuronal and mitochondrial functions in different types of neurons, brain regions, and developmental stages of the CNS. Under pathological conditions, like epileptic seizures, the tight coupling between neuronal activity and mitochondria has devastating effects on mitochondrial function, implying mitochondrial Ca²⁺ overload, synchronous depolarization of the mitochondrial compartment, and enhanced ROS production. This might cause energy failure, release of pro-apoptotic factors, and oxidative damage of lipid membranes and DNA, even in the acute phase of seizure activity. Neuroprotective strategies in epilepsy research might focus on mitochondria-mediated secondary tissue damage. The development of pharmacological tools for protection of mitochondria and ROS scavenging might help to establish adjuvant forms of drug therapy for epilepsy patients.

ACKNOWLEDGMENTS

The authors thank Prof. Dr. Uwe Heinemann for critical discussion and helpful suggestions.

GRANTS

O. Kann is supported by the Deutsche Forschungsgemeinschaft (SFB 507 and SFB 665).

REFERENCES

1. Ames A. CNS energy metabolism as related to function. *Brain Res Brain Res Rev* 34: 42–68, 2000.
2. Amzica F, Steriade M. Neuronal and glial membrane potentials during sleep and paroxysmal oscillations in the neocortex. *J Neurosci* 20: 6648–6665, 2000.

3. **Aubin JE.** Autofluorescence of viable cultured mammalian cells. *J Histochem Cytochem* 27: 36–43, 1979.
4. **Augustine GJ, Santamaria F, Tanaka K.** Local calcium signaling in neurons. *Neuron* 40: 331–346, 2003.
5. **Atkins CM, Sweatt JD.** Reactive oxygen species mediate activity-dependent neuron-glia signaling in output fibers of the hippocampus. *J Neurosci* 19: 7241–7248, 1999.
6. **Avanzini G, Franceschetti S.** Cellular biology of epileptogenesis. *Lancet Neurol* 2: 33–42, 2003.
7. **Avshalumov MV, Chen BT, Koos T, Tepper JM, Rice ME.** Endogenous hydrogen peroxide regulates the excitability of midbrain dopamine neurons via ATP-sensitive potassium channels. *J Neurosci* 25: 4222–4231, 2005.
8. **Babcock DF, Herrington J, Goodwin PC, Park YB, Hille B.** Mitochondrial participation in the intracellular Ca^{2+} network. *J Cell Biol* 136: 833–844, 1997.
9. **Bahr BA, Kessler M, Rivera S, Vanderklish PW, Hall RA, Mutneja MS, Gall C, Hoffman KB.** Stable maintenance of glutamate receptors and other synaptic components in long-term hippocampal slices. *Hippocampus* 5: 425–439, 1995.
10. **Bardo S, Cavazzini MG, Emptage N.** The role of the endoplasmic reticulum Ca^{2+} store in the plasticity of central neurons. *Trends Pharmacol Sci* 27: 78–84, 2006.
11. **Baron KT, Wang GJ, Padua RA, Campbell C, Thayer SA.** NMDA-evoked consumption and recovery of mitochondrially targeted aequorin suggests increased Ca^{2+} uptake by a subset of mitochondria in hippocampal neurons. *Brain Res* 993: 124–132, 2003.
12. **Baysal K, Jung DW, Gunter KK, Gunter TE, Brierley GP.** Na^{+} -dependent Ca^{2+} efflux mechanism of heart mitochondria is not a passive $Ca^{2+}/2Na^{+}$ exchanger. *Am J Physiol Cell Physiol* 266: C800–C808, 1994.
13. **Bengzon J, Mohapel P, Ekdahl CT, Lindvall O.** Neuronal apoptosis after brief and prolonged seizures. *Prog Brain Res* 135: 111–119, 2002.
14. **Berger F, Ramirez-Hernandez MH, Ziegler M.** The new life of a centenarian: signalling functions of NAD(P). *Trends Biochem Sci* 29: 111–118, 2004.
15. **Bernardi P.** Mitochondrial transport of cations: channels, exchangers, and permeability transition. *Physiol Rev* 79: 1127–1155, 1999.
16. **Billups B, Forsythe ID.** Presynaptic mitochondrial calcium sequestration influences transmission at mammalian central synapses. *J Neurosci* 22: 5840–5847, 2002.
17. **Bindokas VP, Lee CC, Colmers WF, Miller RJ.** Changes in mitochondrial function resulting from synaptic activity in the rat hippocampal slice. *J Neurosci* 18: 4570–4587, 1998.
18. **Bindokas VP, Jordan J, Lee CC, Miller RJ.** Superoxide production in rat hippocampal neurons: selective imaging with hydroethidine. *J Neurosci* 16: 1324–1336, 1996.
19. **Bito L, Davson H, Levin E, Murray M, Snider N.** The concentrations of free amino acids and other electrolytes in cerebrospinal fluid, in vivo dialysate of brain, and blood plasma of the dog. *J Neurochem* 13: 1057–1067, 1966.
20. **Brand MD.** The stoichiometry of the exchange catalysed by the mitochondrial calcium/sodium antiporter. *Biochem J* 229: 161–166, 1985.
21. **Brennan AM, Connor JA, Shuttleworth CW.** NAD(P)H fluorescence transients after synaptic activity in brain slices: predominant role of mitochondrial function. *J Cereb Blood Flow Metab* 26: 1389–1406, 2006.
22. **Brocard JB, Tassetto M, Reynolds IJ.** Quantitative evaluation of mitochondrial calcium content in rat cortical neurones following a glutamate stimulus. *J Physiol* 531: 793–805, 2001.
23. **Brodin L, Bakeeva L, Shupliakov O.** Presynaptic mitochondria and the temporal pattern of neurotransmitter release. *Philos Trans R Soc Lond B Biol Sci* 354: 365–372, 1999.
24. **Brookes PS, Yoon Y, Robotham JL, Anders MW, Sheu SS.** Calcium, ATP, and ROS: a mitochondrial love-hate triangle. *Am J Physiol Cell Physiol* 287: C817–C833, 2004.
25. **Brown GC.** Regulation of mitochondrial respiration by nitric oxide inhibition of cytochrome *c* oxidase. *Biochim Biophys Acta* 1504: 46–57, 2001.
26. **Brown LA, Key BJ, Lovick TA.** Bio-imaging of nitric oxide-producing neurones in slices of rat brain using 4,5-diaminofluorescein. *J Neurosci Methods* 92: 101–110, 1999.
27. **Brown MR, Sullivan PG, Geddes JW.** Synaptic mitochondria are more susceptible to Ca^{2+} overload than nonsynaptic mitochondria. *J Biol Chem* 281: 11658–11668, 2006.
28. **Brustovetsky N, Dubinsky JM.** Limitations of cyclosporin A inhibition of the permeability transition in CNS mitochondria. *J Neurosci* 20: 8229–8237, 2000.
29. **Buckman JF, Reynolds IJ.** Spontaneous changes in mitochondrial membrane potential in cultured neurons. *J Neurosci* 21: 5054–5065, 2001.
30. **Budd SL, Castilho RF, Nicholls DG.** Mitochondrial membrane potential and hydroethidine-monitored superoxide generation in cultured cerebellar granule cells. *FEBS Lett* 415: 21–24, 1997.
31. **Burette A, Zabel U, Weinberg RJ, Schmidt HH, Valtschanoff JG.** Synaptic localization of nitric oxide synthase and soluble guanylyl cyclase in the hippocampus. *J Neurosci* 22: 8961–8970, 2002.
32. **Caesar K, Akgoren N, Mathiesen C, Lauritzen M.** Modification of activity-dependent increases in cerebellar blood flow by extracellular potassium in anaesthetized rats. *J Physiol* 520: 281–292, 1999.
33. **Carriedo SG, Sensi SL, Yin HZ, Weiss JH.** AMPA exposures induce mitochondrial Ca^{2+} overload and ROS generation in spinal motor neurons in vitro. *J Neurosci* 20: 240–250, 2000.
34. **Casse R, Rowe CC, Newton M, Berlangieri SU, Scott AM.** Positron emission tomography and epilepsy. *Mol Imaging Biol* 4: 338–351, 2002.
35. **Cavalheiro EA, Leite JP, Bortolotto ZA, Turski WA, Ikonomidou C, Turski L.** Long-term effects of pilocarpine in rats: structural damage of the brain triggers kindling and spontaneous recurrent seizures. *Epilepsia* 32: 778–782, 1991.
36. **Chance B, Cohen P, Jöbsis F, Schoener B.** Intracellular oxidation-reduction states in vivo. *Science* 137: 499–508, 1962.
37. **Chen H, Chan DC.** Emerging functions of mammalian mitochondrial fusion and fission. *Hum Mol Genet* 2: R283–R289, 2005.
38. **Chih CP, Roberts EL Jr.** Energy substrates for neurons during neural activity: a critical review of the astrocyte-neuron lactate shuttle hypothesis. *J Cereb Blood Flow Metab* 23: 1263–1281, 2003.
39. **Chinopoulos C, Adam-Vizi V.** Calcium, mitochondria and oxidative stress in neuronal pathology. Novel aspects of an enduring theme. *FEBS J* 273: 433–450, 2006.
40. **Chinopoulos C, Starkov AA, Fiskum G.** Cyclosporin A-insensitive permeability transition in brain mitochondria: inhibition by 2-aminoethoxydiphenyl borate. *J Biol Chem* 278: 27382–27389, 2003.
41. **Clements JD, Lester RA, Tong G, Jahr CE, Westbrook GL.** The time course of glutamate in the synaptic cleft. *Science* 258: 1498–1501, 1992.
42. **Colegrove SL, Albrecht MA, Friel DD.** Quantitative analysis of mitochondrial Ca^{2+} uptake and release pathways in sympathetic neurons. Reconstruction of the recovery after depolarization-evoked $[Ca^{2+}]_i$ elevations. *J Gen Physiol* 115: 371–388, 2000.
43. **Colegrove SL, Albrecht MA, Friel DD.** Dissection of mitochondrial Ca^{2+} uptake and release fluxes in situ after depolarization-evoked $[Ca^{2+}]_i$ elevations in sympathetic neurons. *J Gen Physiol* 115: 351–370, 2000.
44. **Collins TJ, Berridge MJ, Lipp P, Bootman MD.** Mitochondria are morphologically and functionally heterogeneous within cells. *EMBO J* 21: 1616–1627, 2002.
45. **David G, Talbot J, Barrett EF.** Quantitative estimate of mitochondrial $[Ca^{2+}]_i$ in stimulated motor nerve terminals. *Cell Calcium* 33: 197–206, 2003.
46. **David G, Barrett EF.** Mitochondrial Ca^{2+} uptake prevents desynchronization of quantal release and minimizes depletion during repetitive stimulation of mouse motor nerve terminals. *J Physiol* 548: 425–438, 2003.
47. **Davis AF, Clayton DA.** In situ localization of mitochondrial DNA replication in intact mammalian cells. *J Cell Biol* 135: 883–893, 1996.
48. **Dawson VL, Dawson TM.** Deadly conversations: nuclear-mitochondrial cross-talk. *J Bioenerg Biomembr* 36: 287–294, 2004.
49. **Dedov VN, Roufogalis BD.** Organisation of mitochondria in living sensory neurons. *FEBS Lett* 456: 171–174, 1999.
50. **De Vos KJ, Sable J, Miller KE, Sheetz MP.** Expression of phosphatidylinositol (4,5) bisphosphate-specific pleckstrin homology domains alters direction but not the level of axonal transport of mitochondria. *Mol Biol Cell* 14: 3636–3649, 2003.
51. **Dittman JS, Kreitzer AC, Regehr WG.** Interplay between facilitation, depression, and residual calcium at three presynaptic terminals. *J Neurosci* 20: 1374–1385, 2000.

52. Dreier JP, Kleeberg J, Petzold G, Priller J, Windmüller O, Orzechowski HD, Lindauer U, Heinemann U, Einhäupl KM, Dirnagl U. Endothelin-1 potently induces Leao's cortical spreading depression in vivo in the rat: a model for an endothelial trigger of migrainous aura? *Brain* 125: 102–112, 2002.
53. Dreier JP, Korner K, Gorner A, Lindauer U, Weih M, Villringer A, Dirnagl U. Nitric oxide modulates the CBF response to increased extracellular potassium. *J Cereb Blood Flow Metab* 15: 914–919, 1995.
54. Dringen R. Metabolism and functions of glutathione in brain. *Prog Neurobiol* 62: 649–671, 2000.
55. Duchen MR. Mitochondria in health and disease: perspectives on a new mitochondrial biology. *Mol Aspects Med* 25: 365–451, 2004.
56. Duchen MR. Ca^{2+} -dependent changes in the mitochondrial energetics in single dissociated mouse sensory neurons. *Biochem J* 283: 41–50, 1992.
57. Dugan LL, Sensi SL, Canzoniero LM, Handran SD, Rothman SM, Lin TS, Goldberg MP, Choi DW. Mitochondrial production of reactive oxygen species in cortical neurons following exposure to *N*-methyl-D-aspartate. *J Neurosci* 15: 6377–6388, 1995.
58. Dykens JA. Isolated cerebral and cerebellar mitochondria produce free radicals when exposed to elevated Ca^{2+} and Na^+ : implications for neurodegeneration. *J Neurochem* 63: 584–591, 1994.
59. Engel J Jr. Surgery for seizures. *N Engl J Med* 334: 647–652, 1996.
60. Erecinska M, Cherian S, Silver IA. Energy metabolism in mammalian brain during development. *Prog Neurobiol* 73: 397–445, 2004.
61. Erecinska M, Nelson D, Silver IA. Metabolic and energetic properties of isolated nerve ending particles (synaptosomes). *Biochim Biophys Acta* 1277: 13–34, 1996.
62. Fiskum G, Murphy AN, Beal MF. Mitochondria in neurodegeneration: acute ischemia and chronic neurodegenerative diseases. *J Cereb Blood Flow Metab* 19: 351–369, 1999.
63. Folbergrova J, He QP, Li PA, Smith ML, Siesjo BK. The effect of alpha-phenyl-*N*-tert-butyl nitron on bioenergetic state in substantia nigra following flurothyl-induced status epilepticus in rats. *Neurosci Lett* 266: 121–124, 1999.
64. Folbergrova J, Ingvar M, Siesjo BK. Metabolic changes in cerebral cortex, hippocampus, and cerebellum during sustained bicuculline-induced seizures. *J Neurochem* 37: 1228–1238, 1981.
65. Foster KA, Beaver CJ, Turner DA. Interaction between tissue oxygen tension and NADH imaging during synaptic stimulation and hypoxia in rat hippocampal slices. *Neuroscience* 132: 645–657, 2005.
66. Frantseva MV, Velazquez JL, Hwang PA, Carlen PL. Free radical production correlates with cell death in an in vitro model of epilepsy. *Eur J Neurosci* 12: 1431–1439, 2000.
67. Frantseva MV, Perez Velazquez JL, Tsoraklidis G, Mendonca AJ, Adamchik Y, Mills LR, Carlen PL, Burnham MW. Oxidative stress is involved in seizure-induced neurodegeneration in the kindling model of epilepsy. *Neuroscience* 97: 431–435, 2000.
68. Friel DD, Tsien RW. An FCCP-sensitive Ca^{2+} store in bullfrog sympathetic neurons and its participation in stimulus-evoked changes in $[Ca^{2+}]_i$. *J Neurosci* 14: 4007–4024, 1994.
69. Gabriel S, Njunting M, Pomper JK, Merschhemke M, Sanabria ER, Eilers A, Kivi A, Zeller M, Meencke HJ, Cavalheiro EA, Heinemann U, Lehmann TN. Stimulus and potassium-induced epileptiform activity in the human dentate gyrus from patients with and without hippocampal sclerosis. *J Neurosci* 24: 10416–10430, 2004.
70. Garcia-Chacon LE, Nguyen KT, David G, Barrett EF. Extrusion of Ca^{2+} from mouse motor terminal mitochondria via a Na^+/Ca^{2+} exchanger increases post-tetanic evoked release. *J Physiol* 574: 663–675, 2006.
71. Gerencser AA, Adam-Vizi V. Mitochondrial Ca^{2+} dynamics reveals limited intramitochondrial Ca^{2+} diffusion. *Biophys J* 88: 698–714, 2005.
72. Gerencser AA, Adam-Vizi V. Selective, high-resolution fluorescence imaging of mitochondrial Ca^{2+} concentration. *Cell Calcium* 30: 311–321, 2001.
73. Ghafourifar P, Richter C. Nitric oxide synthase activity in mitochondria. *FEBS Lett* 418: 291–296, 1997.
74. Gunter TE, Yule DI, Gunter KK, Eliseev RA, Salter JD. Calcium and mitochondria. *FEBS Lett* 567: 96–102, 2004.
75. Gunter KK, Zuscik MJ, Gunter TE. The Na^+ -independent Ca^{2+} efflux mechanism of liver mitochondria is not a passive $Ca^{2+}/2H^+$ exchanger. *J Biol Chem* 266: 21640–21648, 1991.
76. Gunter TE, Pfeiffer DR. Mechanisms by which mitochondria transport calcium. *Am J Physiol Cell Physiol* 258: C755–C786, 1990.
77. Gupta RC, Milatovic D, Dettbarn WD. Depletion of energy metabolites following acetylcholinesterase inhibitor-induced status epilepticus: protection by antioxidants. *Neurotoxicology* 22: 271–282, 2001.
78. Gutierrez R, Heinemann U. Synaptic reorganization in explanted cultures of rat hippocampus. *Brain Res* 815: 304–316, 1999.
79. Hajnoczky G, Robb-Gaspers LD, Seitz MB, Thomas AP. Decoding of cytosolic calcium oscillations in the mitochondria. *Cell* 82: 415–424, 1995.
80. Hansford RG, Zorov D. Role of mitochondrial calcium transport in the control of substrate oxidation. *Mol Cell Biochem* 184: 359–369, 1998.
81. Hattori T, Watanabe K, Uechi Y, Yoshioka H, Ohta Y. Repetitive transient depolarizations of the inner mitochondrial membrane induced by proton pumping. *Biophys J* 88: 2340–2349, 2005.
82. Hauser WA. Incidence and prevalence. In: *Epilepsy: A Comprehensive Textbook*, edited by Engel J Jr and Pedley TA. Philadelphia: Lippincott-Raven, 1997 p. 47–57.
83. Hayakawa Y, Nemoto T, Iino M, Kasai H. Rapid Ca^{2+} -dependent increase in oxygen consumption by mitochondria in single mammalian central neurons. *Cell Calcium* 37: 359–370, 2005.
84. Heinemann U, Schaible HG, Schmidt RF. Changes in extracellular potassium concentration in cat spinal cord in response to innocuous and noxious stimulation of legs with healthy and inflamed knee joints. *Exp Brain Res* 79: 283–292, 1990.
85. Heinemann U, Lux HD, Gutnick MJ. Extracellular free calcium and potassium during paroxysmal activity in the cerebral cortex of the cat. *Exp Brain Res* 27: 237–243, 1977.
86. Heinemann U, Lux HD. Undershoots following stimulus-induced rises of extracellular potassium concentration in cerebral cortex of cat. *Brain Res* 93: 63–76, 1975.
87. Hirase H, Creso J, Buzsaki G. Capillary level imaging of local cerebral blood flow in bicuculline-induced epileptic foci. *Neuroscience* 128: 209–216, 2004.
88. Hollenbeck PJ, Saxton WM. The axonal transport of mitochondria. *J Cell Sci* 118: 5411–5419, 2005.
89. Hongpaisan J, Winters CA, Andrews SB. Strong calcium entry activates mitochondrial superoxide generation, upregulating kinase signaling in hippocampal neurons. *J Neurosci* 24: 10878–10887, 2004.
90. Huang S, Heikal AA, Webb WW. Two-photon fluorescence spectroscopy and microscopy of NAD(P)H and flavoprotein. *Biophys J* 82: 2811–2812, 2002.
91. Huser J, Blatter LA. Fluctuations in mitochondrial membrane potential caused by repetitive gating of the permeability transition pore. *Biochem J* 343: 311–317, 1999.
92. Ichas F, Jouaville LS, Mazat JP. Mitochondria are excitable organelles capable of generating and conveying electrical and calcium signals. *Cell* 89: 1145–1153, 1997.
93. Ingvar M, Siesjo BK. Local blood flow and glucose consumption in the rat brain during sustained bicuculline-induced seizures. *Acta Neurol Scand* 68: 129–144, 1983.
94. Jakobs S. High resolution imaging of live mitochondria. *Biochim Biophys Acta* 1763: 561–575, 2006.
95. Jonas EA, Buchanan J, Kaczmarek LK. Prolonged activation of mitochondrial conductances during synaptic transmission. *Science* 286: 1347–1350, 1999.
96. Jonas E. Regulation of synaptic transmission by mitochondrial ion channels. *J Bioenerg Biomembr* 36: 357–361, 2004.
97. Jöbsis FF, O'Connor M, Vitale A, Vreman H. Intracellular redox changes in functioning cerebral cortex. I. Metabolic effects of epileptiform activity. *J Neurophysiol* 34: 735–749, 1971.
98. Jung DW, Baysal K, Brierley GP. The sodium-calcium antiport of heart mitochondria is not electroneutral. *J Biol Chem* 270: 672–678, 1995.
99. Kadenbach B. Intrinsic and extrinsic uncoupling of oxidative phosphorylation. *Biochim Biophys Acta* 1604: 77–94, 2003.
100. Kaneko K, Itoh K, Berliner LJ, Miyasaka K, Fujii H. Consequences of nitric oxide generation in epileptic-seizure rodent models as studied by in vivo EPR. *Magn Reson Med* 48: 1051–1056, 2002.
101. Kann O, Kovacs R, Njunting M, Behrens CJ, Otahal J, Lehmann TN, Gabriel S, Heinemann U. Metabolic dysfunction during neuronal activation in the ex vivo hippocampus from chronic epileptic rats and humans. *Brain* 128: 2396–2407, 2005.
102. Kann O, Schuchmann S, Buchheim K, Heinemann U. Coupling of neuronal activity and mitochondrial metabolism as revealed by NAD(P)H fluorescence signals in organotypic hippocampal slice cultures of the rat. *Neuroscience* 119: 87–100, 2003.

103. **Kann O, Kovacs R, Heinemann U.** Metabotropic receptor-mediated Ca^{2+} signaling elevates mitochondrial Ca^{2+} and stimulates oxidative metabolism in hippocampal slice cultures. *J Neurophysiol* 90: 613–621, 2003.
104. **Kaplan NO.** The role of pyridine nucleotides in regulating cellular metabolism. *Curr Top Cell Regul* 26: 371–381, 1985.
105. **Kasischke KA, Vishwasrao HD, Fisher PJ, Zipfel WR, Webb WW.** Neural activity triggers neuronal oxidative metabolism followed by astrocytic glycolysis. *Science* 305: 99–103, 2004.
106. **Kato N, Sato S, Yokoyama H, Kayama T, Yoshimura T.** Sequential changes of nitric oxide levels in the temporal lobes of kainic acid-treated mice following application of nitric oxide synthase inhibitors and phenobarbital. *Epilepsy Res* 65: 81–91, 2005.
107. **Keynes RG, Dupont S, Garthwaite J.** Hippocampal neurons in organotypic slice culture are highly resistant to damage by endogenous and exogenous nitric oxide. *Eur J Neurosci* 19: 1163–1173, 2004.
108. **Kim-Han JS, Dugan LL.** Mitochondrial uncoupling proteins in the central nervous system. *Antioxid Redox Signal* 7: 1173–1181, 2005.
109. **Kirichok Y, Krapivinsky G, Clapham DE.** The mitochondrial calcium uniporter is a highly selective ion channel. *Nature* 427: 360–364, 2004.
110. **Kirsch M, De Groot H.** NAD(P)H, a directly operating antioxidant? *FASEB J* 15: 1569–1574, 2001.
111. **Klaidman LK, Mukherjee SK, Adams JD Jr.** Oxidative changes in brain pyridine nucleotides and neuroprotection using nicotinamide. *Biochim Biophys Acta* 1525: 136–148, 2001.
112. **Kovacs R, Kardos J, Heinemann U, Kann O.** Mitochondrial calcium ion and membrane potential transients follow the pattern of epileptiform discharges in hippocampal slice cultures. *J Neurosci* 25: 4260–4269, 2005.
113. **Kovacs R, Schuchmann S, Gabriel S, Kann O, Kardos J, Heinemann U.** Free radical-mediated cell damage after experimental status epilepticus in hippocampal slice cultures. *J Neurophysiol* 88: 2909–2918, 2002.
114. **Kovacs R, Schuchmann S, Gabriel S, Kardos J, Heinemann U.** Ca^{2+} signalling and changes of mitochondrial function during low- Mg^{2+} -induced epileptiform activity in organotypic hippocampal slice cultures. *Eur J Neurosci* 13: 1311–1319, 2001.
115. **Kovacs R, Gutierrez R, Kivi A, Schuchmann S, Gabriel S, Heinemann U.** Acute cell damage after low Mg^{2+} -induced epileptiform activity in organotypic hippocampal slice cultures. *Neuroreport* 10: 207–213, 1999.
116. **Kreisman NR, Magee JC, Brizzee BL.** Relative hypoperfusion in rat cerebral cortex during recurrent seizures. *J Cereb Blood Flow Metab* 11: 77–87, 1991.
117. **Kudin AP, Bimpong-Buta NY, Vielhaber S, Elger CE, Kunz WS.** Characterization of superoxide-producing sites in isolated brain mitochondria. *J Biol Chem* 279: 4127–4135, 2004.
118. **Kuhl DE, Engel J Jr, Phelps ME, Selin C.** Epileptic patterns of local cerebral metabolism and perfusion in humans determined by emission computed tomography of ^{18}F FDG and ^{13}N H_3 . *Ann Neurol* 8: 348–360, 1980.
119. **Kunz WS, Kudin AP, Vielhaber S, Blumcke I, Zschratler W, Schramm J, Beck H, Elger CE.** Mitochondrial complex I deficiency in the epileptic focus of patients with temporal lobe epilepsy. *Ann Neurol* 48: 766–773, 2000.
120. **Kunz WS, Goussakov IV, Beck H, Elger CE.** Altered mitochondrial oxidative phosphorylation in hippocampal slices of kainate-treated rats. *Brain Res* 826: 236–242, 1999.
121. **Kunz WS, Gellerich FN.** Quantification of the content of fluorescent flavoproteins in mitochondria from liver, kidney cortex, skeletal muscle, and brain. *Biochem Med Metab Biol* 50: 103–110, 1993.
122. **Lacza Z, Pankotai E, Csordas A, Gero D, Kiss L, Horvath EM, Kollai M, Busija DW, Szabo C.** Mitochondrial NO and reactive nitrogen species production: does mtNOS exist? *Nitric Oxide* 14: 162–168, 2006.
123. **Ladewig T, Kloppenburg P, Lalley PM, Zipfel WR, Webb WW, Keller BU.** Spatial profiles of store-dependent calcium release in motoneurons of the nucleus hypoglossus from newborn mouse. *J Physiol* 547: 775–787, 2003.
124. **Leino RL, Gerhart DZ, van Bueren AM, McCall AL, Drewes LR.** Ultrastructural localization of GLUT 1 and GLUT 3 glucose transporters in rat brain. *J Neurosci Res* 49: 617–626, 1997.
125. **Lewis DV, Schuette WH.** NADH fluorescence and $[\text{K}^+]_o$ changes during hippocampal electrical stimulation. *J Neurophysiol* 38: 405–417, 1975.
126. **Leybaert L.** Neurobarrier coupling in the brain: a partner of neurovascular and neurometabolic coupling? *J Cereb Blood Flow Metab* 25: 2–16, 2005.
127. **Li CL, McIlwain H.** Maintenance of resting membrane potentials in slices of mammalian cerebral cortex and other tissues in vitro. *J Physiol* 139: 178–190, 1957.
128. **Li Z, Okamoto K, Hayashi Y, Sheng M.** The importance of dendritic mitochondria in the morphogenesis and plasticity of spines and synapses. *Cell* 119: 873–887, 2004.
129. **Liang LP, Patel M.** Seizure-induced changes in mitochondrial redox status. *Free Radic Biol Med* 40: 316–322, 2006.
130. **Liang LP, Patel M.** Mitochondrial oxidative stress and increased seizure susceptibility in $\text{Sod}2^{-/+}$ mice. *Free Radic Biol Med* 36: 542–554, 2004.
131. **Liang LP, Ho YS, Patel M.** Mitochondrial superoxide production in kainate-induced hippocampal damage. *Neuroscience* 101: 563–570, 2000.
132. **Lipton P, Robacker K.** Glycolysis and brain function: $[\text{K}^+]_o$ stimulation of protein synthesis and K^+ uptake require glycolysis. *Fed Proc* 42: 2875–2880, 1983.
133. **Lipton P.** Effects of membrane depolarization on nicotinamide nucleotide fluorescence in brain slices. *Biochem J* 136: 999–1009, 1973.
134. **Litsky ML, Pfeiffer DR.** Regulation of the mitochondrial Ca^{2+} uniporter by external adenine nucleotides: the uniporter behaves like a gated channel which is regulated by nucleotides and divalent cations. *Biochemistry* 36: 7071–7080, 1997.
135. **Loew LM, Carrington W, Tuft RA, Fay FS.** Physiological cytosolic Ca^{2+} transients evoke concurrent mitochondrial depolarizations. *Proc Natl Acad Sci USA* 91: 12579–12583, 1994.
136. **Loew LM, Tuft RA, Carrington W, Fay FS.** Imaging in five dimensions: time-dependent membrane potentials in individual mitochondria. *Biophys J* 65: 2396–2407, 1993.
137. **Lux HD, Heinemann U, Dietzel I.** Ionic changes and alterations in the size of the extracellular space during epileptic activity. *Adv Neurol* 44: 619–639, 1986.
138. **Lux HD, Neher E.** The equilibration time course of $(\text{K}^+)_o$ in cat cortex. *Exp Brain Res* 17: 190–205, 1973.
139. **Magistretti PJ, Pellerin L.** Cellular mechanisms of brain energy metabolism and their relevance to functional brain imaging. *Philos Trans R Soc Lond B Biol Sci* 354: 1155–1163, 1999.
140. **Malonek D, Dirnagl U, Lindauer U, Yamada K, Kanno I, Grinvald A.** Vascular imprints of neuronal activity: relationships between the dynamics of cortical blood flow, oxygenation, and volume changes following sensory stimulation. *Proc Natl Acad Sci USA* 94: 14826–14831, 1997.
141. **Margerison JH, Corsellis JA.** Epilepsy and the temporal lobes. A clinical, electroencephalographic and neuropathological study of the brain in epilepsy, with particular reference to the temporal lobes. *Brain* 89: 499–530, 1966.
142. **Matlib MA, Zhou Z, Knight S, Ahmed S, Choi KM, Krause-Bauer J, Phillips R, Altschuld R, Katsube Y, Sperelakis N, Bers DM.** Oxygen-bridged dinuclear ruthenium amine complex specifically inhibits Ca^{2+} uptake into mitochondria in vitro and in situ in single cardiac myocytes. *J Biol Chem* 273: 10223–10231, 1998.
143. **Mattiasson G, Friberg H, Hansson M, Elmer E, Wieloch T.** Flow cytometric analysis of mitochondria from CA1 and CA3 regions of rat hippocampus reveals differences in permeability transition pore activation. *J Neurochem* 87: 532–544, 2003.
144. **Mayevsky A, Chance B.** Metabolic responses of the awake cerebral cortex to anoxia hypoxia spreading depression and epileptiform activity. *Brain Res* 98: 149–165, 1975.
145. **McCormack JG, Halestrap AP, Denton RM.** Role of calcium ions in regulation of mammalian intramitochondrial metabolism. *Physiol Rev* 70: 391–425, 1990.
146. **Medler K, Gleason EL.** Mitochondrial Ca^{2+} buffering regulates synaptic transmission between retinal amacrine cells. *J Neurophysiol* 87: 1426–1439, 2002.
147. **Meldrum BS, Nilsson B.** Cerebral blood flow and metabolic rate early and late in prolonged epileptic seizures induced in rats by bicuculline. *Brain* 99: 523–542, 1976.
148. **Miller KE, Smetz MP.** Axonal mitochondrial transport and potential are correlated. *J Cell Sci* 117: 2791–2804, 2004.
149. **Mironov SL.** Spontaneous and evoked neuronal activities regulate movements of single neuronal mitochondria. *Synapse* 59: 403–411, 2006.

150. Mironov SL, Richter DW. Oscillations and hypoxic changes of mitochondrial variables in neurons of the brainstem respiratory centre of mice. *J Physiol* 533: 227–236, 2001.
151. Mitchell P. *Chemiosmotic Coupling in Oxidative and Photosynthetic Phosphorylation*. Bodmin, UK: Glynn Research, 1966.
152. Mody I, Lambert JD, Heinemann U. Low extracellular magnesium induces epileptiform activity and spreading depression in rat hippocampal slices. *J Neurophysiol* 57: 869–888, 1987.
153. Morris RL, Hollenbeck PJ. Axonal transport of mitochondria along microtubules and F-actin in living vertebrate neurons. *J Cell Biol* 131: 1315–1326, 1995.
154. Müller M, Mironov SL, Ivannikov MV, Schmidt J, Richter DW. Mitochondrial organization and motility probed by two-photon microscopy in cultured mouse brainstem neurons. *Exp Cell Res* 303: 114–127, 2005.
155. Murchison D, Zawieja DC, Griffith WH. Reduced mitochondrial buffering of voltage-gated calcium influx in aged rat basal forebrain neurons. *Cell Calcium* 36: 61–75, 2004.
156. Newman EA. Glial cell regulation of extracellular potassium. In: *Neuroglia*, edited by Kettenmann H, Ransom BR. New York: Oxford Univ. Press, 1995, p. 717–731.
157. Nicholls DG. Simultaneous monitoring of ionophore- and inhibitor-mediated plasma and mitochondrial membrane potential changes in cultured neurons. *J Biol Chem* 281: 14864–14874, 2006.
158. Nicholls DG, Budd SL. Mitochondria and neuronal survival. *Physiol Rev* 80: 315–360, 2000.
159. Nimchinsky EA, Yasuda R, Oertner TG, Svoboda K. The number of glutamate receptors opened by synaptic stimulation in single hippocampal spines. *J Neurosci* 24: 2054–2064, 2004.
160. Niwa K, Araki E, Morham SG, Ross ME, Iadecola C. Cyclooxygenase-2 contributes to functional hyperemia in whisker-barrel cortex. *J Neurosci* 20: 763–770, 2000.
161. Norenberg MD. Astroglial dysfunction in hepatic encephalopathy. *Metab Brain Dis* 13: 319–335, 1998.
162. Orth M, Schapira AH. Mitochondria and degenerative disorders. *Am J Med Genet* 106: 27–36, 2001.
163. Overly CC, Rieff HI, Hollenbeck PJ. Organelle motility and metabolism in axons vs dendrites of cultured hippocampal neurons. *J Cell Sci* 109: 971–980, 1996.
164. Pacher P, Thomas AP, Hajnoczky G. Ca²⁺ marks: miniature calcium signals in single mitochondria driven by ryanodine receptors. *Proc Natl Acad Sci USA* 99: 2380–2385, 2002.
165. Papa S, Skulachev VP. Reactive oxygen species, mitochondria, apoptosis and aging. *Mol Cell Biochem* 174: 305–319, 1997.
166. Pardo B, Contreras L, Serrano A, Ramos M, Kobayashi K, Iijima M, Saheki T, Satrustegui J. Essential role of aralar in the transduction of small Ca²⁺ signals to neuronal mitochondria. *J Biol Chem* 281: 1039–1047, 2006.
167. Pardridge WM. Blood-brain barrier transport of glucose, free fatty acids, and ketone bodies. *Adv Exp Med Biol* 291: 43–53, 1991.
168. Patel M. Mitochondrial dysfunction and oxidative stress: cause and consequence of epileptic seizures. *Free Radic Biol Med* 37: 1951–1962, 2004.
169. Peng TI, Greenamyre JT. Privileged access to mitochondria of calcium influx through N-methyl-D-aspartate receptors. *Mol Pharmacol* 53: 974–980, 1998.
170. Peterson SL, Morrow D, Liu S, Liu KJ. Hydroethidine detection of superoxide production during the lithium-pilocarpine model of status epilepticus. *Epilepsy Res* 49: 226–238, 2002.
171. Pfeuffer J, Tkac I, Gruetter R. Extracellular-intracellular distribution of glucose and lactate in the rat brain assessed noninvasively by diffusion-weighted ¹H nuclear magnetic resonance spectroscopy in vivo. *J Cereb Blood Flow Metab* 20: 736–746, 2000.
172. Pitkänen A, Sutula TP. Is epilepsy a progressive disorder? Prospects for new therapeutic approaches in temporal-lobe epilepsy. *Lancet Neurol* 1: 173–181, 2002.
173. Pitter JG, Maechler P, Wollheim CB, Spat A. Mitochondria respond to Ca²⁺ already in the submicromolar range: correlation with redox state. *Cell Calcium* 31: 97–104, 2002.
174. Pivovarova NB, Pozzo-Miller LD, Hongpaisan J, Andrews SB. Correlated calcium uptake and release by mitochondria and endoplasmic reticulum of CA3 hippocampal dendrites after afferent synaptic stimulation. *J Neurosci* 22: 10653–10661, 2002.
175. Pivovarova NB, Hongpaisan J, Andrews SB, Friel DD. Depolarization-induced mitochondrial Ca accumulation in sympathetic neurons: spatial and temporal characteristics. *J Neurosci* 19: 6372–6384, 1999.
176. Pomper JK, Haack S, Petzold GC, Buchheim K, Gabriel S, Hoffmann U, Heinemann U. Repetitive spreading depression-like events result in cell damage in juvenile hippocampal slice cultures maintained in normoxia. *J Neurophysiol* 95: 355–368, 2006.
177. Popov V, Medvedev NI, Davies HA, Stewart MG. Mitochondria form a filamentous reticular network in hippocampal dendrites but are present as discrete bodies in axons: a three-dimensional ultrastructural study. *J Comp Neurol* 492: 50–65, 2005.
178. Pralong WF, Spat A, Wollheim CB. Dynamic pacing of cell metabolism by intracellular Ca²⁺ transients. *J Biol Chem* 269: 27310–27314, 1994.
179. Ravagnan L, Roumier T, Kroemer G. Mitochondria, the killer organelles and their weapons. *J Cell Physiol* 192: 131–137, 2002.
180. Reinert KC, Dunbar RL, Gao W, Chen G, Ebner TJ. Flavoprotein autofluorescence imaging of neuronal activation in the cerebellar cortex in vivo. *J Neurophysiol* 92: 199–211, 2004.
181. Reynolds IJ, Hastings TG. Glutamate induces the production of reactive oxygen species in cultured forebrain neurons following NMDA receptor activation. *J Neurosci* 15: 3318–3327, 1995.
182. Rintoul GL, Filiano AJ, Brocard JB, Kress GJ, Reynolds IJ. Glutamate decreases mitochondrial size and movement in primary forebrain neurons. *J Neurosci* 23: 7881–7888, 2003.
183. Rizzuto R, Pozzan T. Microdomains of intracellular Ca²⁺: molecular determinants and functional consequences. *Physiol Rev* 86: 369–408, 2006.
184. Rosenthal M, Jöbsis FF. Intracellular redox changes in functioning cerebral cortex. II. Effects of direct cortical stimulation. *J Neurophysiol* 34: 750–762, 1971.
185. Rowland KC, Irby NK, Spirou GA. Specialized synapse-associated structures within the calyx of Held. *J Neurosci* 20: 9135–9144, 2000.
186. Sarti P, Lendaro E, Ippoliti R, Bellelli A, Benedetti PA, Brunori M. Modulation of mitochondrial respiration by nitric oxide: investigation by single cell fluorescence microscopy. *FASEB J* 13: 191–197, 1999.
187. Schapira AH. Mitochondrial involvement in Parkinson's disease, Huntington's disease, hereditary spastic paraplegia and Friedreich's ataxia. *Biochim Biophys Acta* 1410: 159–170, 1999.
188. Schousboe A, Sarup A, Bak LK, Waagepetersen HS, Larsson OM. Role of astrocytic transport processes in glutamatergic and GABAergic neurotransmission. *Neurochem Int* 45: 521–527, 2004.
189. Schuchmann S, Albrecht D, Heinemann U, von Bohlen und Halbach O. Nitric oxide modulates low-Mg²⁺-induced epileptiform activity in rat hippocampal-entorhinal cortex slices. *Neurobiol Dis* 11: 96–105, 2002.
190. Schuchmann S, Kovacs R, Kann O, Heinemann U, Buchheim K. Monitoring NAD(P)H autofluorescence to assess mitochondrial metabolic functions in rat hippocampal-entorhinal cortex slices. *Brain Res Brain Res Protoc* 7: 267–276, 2001.
191. Schuchmann S, Luckermann M, Kulik A, Heinemann U, Ballanyi K. Ca²⁺- and metabolism-related changes of mitochondrial potential in voltage-clamped CA1 pyramidal neurons in situ. *J Neurophysiol* 83: 1710–1721, 2000.
192. Schuchmann S, Buchheim K, Meierkord H, Heinemann U. A relative energy failure is associated with low-Mg²⁺ but not with 4-aminopyridine induced seizure-like events in entorhinal cortex. *J Neurophysiol* 81: 399–403, 1999.
193. Schuchmann S, Müller W, Heinemann U. Altered Ca²⁺ signaling and mitochondrial deficiencies in hippocampal neurons of trisomy 16 mice: a model of Down's syndrome. *J Neurosci* 18: 7216–7231, 1998.
194. Schurr A, Payne RS, Miller JJ, Rigor BM. Brain lactate is an obligatory aerobic energy substrate for functional recovery after hypoxia: further in vitro validation. *J Neurochem* 69: 423–426, 1997.
195. Schwartzkroin PA, Andersen P. Glutamic acid sensitivity of dendrites in hippocampal slices in vitro. *Adv Neurol* 12: 45–51, 1975.
196. Shepherd GM, Harris KM. Three-dimensional structure and composition of CA3→CA1 axons in rat hippocampal slices: implications for presynaptic connectivity and compartmentalization. *J Neurosci* 18: 8300–8310, 1998.
197. Shuttleworth CW, Brennan AM, Connor JA. NAD(P)H fluorescence imaging of postsynaptic neuronal activation in murine hippocampal slices. *J Neurosci* 23: 3196–3208, 2003.
198. Siesjö BK. *Brain Energy Metabolism*. New York: Wiley, 1978.

199. **Silver I, Erecinska M.** Oxygen and ion concentrations in normoxic and hypoxic brain cells. *Adv Exp Med Biol* 454: 7–16, 1998.
200. **Simard M, Nedergaard M.** The neurobiology of glia in the context of water and ion homeostasis. *Neuroscience* 129: 877–896, 2004.
201. **Skulachev VP, Bakeeva LE, Chernyak BV, Domnina LV, Minin AA, Pletjushkina OY, Saprunova VB, Skulachev IV, Tsyplenkova VG, Vasiliev JM, Yaguzhinsky LS, Zorov DB.** Thread-grain transition of mitochondrial reticulum as a step of mitoptosis and apoptosis. *Mol Cell Biochem* 256–257: 341–358, 2004.
202. **Skulachev VP.** Mitochondrial filaments and clusters as intracellular power-transmitting cables. *Trends Biochem Sci* 26: 23–29, 2001.
203. **Smith SM, Bergsman JB, Harata NC, Scheller RH, Tsien RW.** Recordings from single neocortical nerve terminals reveal a nonselective cation channel activated by decreases in extracellular calcium. *Neuron* 41: 243–256, 2004.
204. **Sparagna GC, Gunter KK, Sheu SS, Gunter TE.** Mitochondrial calcium uptake from physiological-type pulses of calcium. A description of the rapid uptake mode. *J Biol Chem* 270: 27510–27515, 1995.
205. **Starkov AA, Fiskum G, Chinopoulos C, Lorenzo BJ, Browne SE, Patel MS, Beal MF.** Mitochondrial alpha-ketoglutarate dehydrogenase complex generates reactive oxygen species. *J Neurosci* 24: 7779–7788, 2004.
206. **Starkov AA, Fiskum G.** Regulation of brain mitochondrial H₂O₂ production by membrane potential and NAD(P)H redox state. *J Neurochem* 86: 1101–1107, 2003.
207. **Stoppini L, Buchs PA, Muller D.** A simple method for organotypic cultures of nervous tissue. *J Neurosci Methods* 37: 173–182, 1991.
208. **Sutula T, Cascino G, Cavazos J, Parada I, Ramirez L.** Mossy fiber synaptic reorganization in the epileptic human temporal lobe. *Ann Neurol* 26: 321–330, 1989.
209. **Tanaka S, Sako K, Tanaka T, Nishihara I, Yonemasu Y.** Uncoupling of local blood flow and metabolism in the hippocampal CA3 in kainic acid-induced limbic seizure status. *Neuroscience* 36: 339–348, 1990.
210. **Tang Y, Zucker RS.** Mitochondrial involvement in post-tetanic potentiation of synaptic transmission. *Neuron* 18: 483–491, 1997.
211. **Taylor CP, Weber ML, Gaughan CL, Lehning EJ, LoPachin RM.** Oxygen/glucose deprivation in hippocampal slices: altered intraneuronal elemental composition predicts structural and functional damage. *J Neurosci* 19: 619–629, 1999.
212. **Traaseth N, Elfering S, Solien J, Haynes V, Giulivi C.** Role of calcium signaling in the activation of mitochondrial nitric oxide synthase and citric acid cycle. *Biochim Biophys Acta* 1658: 64–71, 2004.
213. **Ueda Y, Yokoyama H, Nakajima A, Tokumaru J, Doi T, Mitsuyama Y.** Glutamate excess and free radical formation during and following kainic acid-induced status epilepticus. *Exp Brain Res* 147: 219–226, 2002.
214. **Verstreken P, Ly CV, Venken KJ, Koh TW, Zhou Y, Bellen HJ.** Synaptic mitochondria are critical for mobilization of reserve pool vesicles at *Drosophila* neuromuscular junctions. *Neuron* 47: 365–378, 2005.
215. **Villringer A, Dirnagl U.** Coupling of brain activity and cerebral blood flow: basis of functional neuroimaging. *Cerebrovasc Brain Metab Rev* 7: 240–276, 1995.
216. **Votyakova TV, Reynolds IJ.** ΔΨ_m-Dependent and -independent production of reactive oxygen species by rat brain mitochondria. *J Neurochem* 79: 266–277, 2001.
217. **Vovenko E.** Distribution of oxygen tension on the surface of arterioles, capillaries and venules of brain cortex and in tissue in normoxia: an experimental study on rats. *Pflügers Arch* 437: 617–623, 1999.
218. **Wallace DC.** A mitochondrial paradigm of metabolic and degenerative diseases, aging, and cancer: a dawn for evolutionary medicine. *Annu Rev Genet* 39: 359–407, 2005.
219. **Wang GJ, Thayer SA.** NMDA-induced calcium loads recycle across the mitochondrial inner membrane of hippocampal neurons in culture. *J Neurophysiol* 87: 740–749, 2002.
220. **Wang GJ, Thayer SA.** Sequestration of glutamate-induced Ca²⁺ loads by mitochondria in cultured rat hippocampal neurons. *J Neurophysiol* 76: 1611–1621, 1996.
221. **White RJ, Reynolds IJ.** Mitochondria and Na⁺/Ca²⁺ exchange buffer glutamate-induced calcium loads in cultured cortical neurons. *J Neurosci* 15: 1318–1328, 1995.
222. **White RL, Wittenberg BA.** Effects of calcium on mitochondrial NAD(P)H in paced rat ventricular myocytes. *Biophys J* 69: 2790–2799, 1995.
223. **Wimmer VC, Horstmann H, Groh A, Kuner T.** Donut-like topology of synaptic vesicles with a central cluster of mitochondria wrapped into membrane protrusions: a novel structure-function module of the adult calyx of Held. *J Neurosci* 26: 109–116, 2006.
224. **Xiong J, Verkhratsky A, Toescu EC.** Changes in mitochondrial status associated with altered Ca²⁺ homeostasis in aged cerebellar granule neurons in brain slices. *J Neurosci* 22: 10761–10771, 2002.
225. **Yaffe MP.** Dynamic mitochondria. *Nat Cell Biol* 1: E149–E150, 1999.
226. **Yi M, Weaver D, Hajnoczky G.** Control of mitochondrial motility and distribution by the calcium signal: a homeostatic circuit. *J Cell Biol* 167: 661–672, 2004.
227. **Zenisek D, Matthews G.** The role of mitochondria in presynaptic calcium handling at a ribbon synapse. *Neuron* 25: 229–237, 2000.
228. **Zimmer J, Gahwiler BH.** Cellular and connective organization of slice cultures of the rat hippocampus and fascia dentata. *J Comp Neurol* 228: 432–446, 1984.
229. **Zonta M, Angulo MC, Gobbo S, Rosengarten B, Hossmann KA, Pozzan T, Carmignoto G.** Neuron-to-astrocyte signaling is central to the dynamic control of brain microcirculation. *Nat Neurosci* 6: 43–50, 2003.
230. **Zoratti M, Szabo I.** The mitochondrial permeability transition. *Biochim Biophys Acta* 1241: 139–176, 1995.
231. **Zorov DB, Kobrinsky E, Juhaszova M, Sollott SJ.** Examining intracellular organelle function using fluorescent probes: from animalcules to quantum dots. *Circ Res* 95: 239–252, 2004.